Time scales and existence of time holes in non-transparent media

Harald Reiss

Department of Physics
University of Wuerzburg, Am Hubland, D-97074 Wuerzburg, FRG

harald.reiss@physik.uni-wuerzburg.de

Abstract

The analysis presented in this paper applies to experimental situations where observers or objects to be studied, all at stationary positions, are located in environments the optical thickness of which is strongly different. Non-transparent media comprise thin metallic films, packed or fluidised beds, superconductors, the Earth's crust, and even dark clouds and other cosmological objects. The analysis applies mapping functions that correlate physical events, e, in non-transparent media, with their images, f(e), tentatively located on standard physical time scale. The analysis demonstrates, however, that physical time, in its rigorous sense, does not exist under non-transparency conditions. A proof of this conclusion is attempted in three steps: i) the theorem "there is no time without space and events" is accepted, (ii) images f[e(**s**,t)] do not constitute a dense, uncountably infinite set, and (iii) sets of images that are not uncountably infinite do not create physical time but only time-like sequences. As a consequence, mapping f[e(**s**,t)] in non-transparent space does not create physical analogues to the mathematical structure of the ordered, dense half-set R^+ of real numbers, and reverse mapping, f^{-1}f[e(**s**,t)], the mathematical inverse problem, would not allow unique identification and reconstruction of original events from their images. In these cases, causality as well as invariance of physical processes under time reversal, might be violated. An interesting problem is whether temporal cloaking (a time hole) in a transparent medium, as very recently reported in the literature, can be explained by the present analysis. Existence of time holes could perhaps be possible, not in transparent but in non-transparent media, as follows from the sequence of images, f[e(**s**,t)], that is not uncountably infinite, in contrast to R^+. Impacts are expected for understanding physical diffusion-like, radiative transfer processes and stability models to protect superconductors against quenchs. There might be impacts also in relativity, quantum mechanics, nuclear decay, or in systems close to their phase transitions. The analysis is not restricted to objects of laboratory dimensions.

Keywords

Non-transparency, radiative transfer, disturbance, physical time, inverse problem, time hole, superconductor

1 Introduction

The analysis presented in this paper is focussed on experimental situations where observers or objects to be studied, all at stationary positions, are located in separate physical environments the optical thickness, or the scattering and absorption/remission properties of which, are strongly different. By their large optical thickness, non-transparent media are clearly distinguished from their transparent counterparts. For the following discussion, it is helpful to first recall basic properties of *transparency* before we will discuss existence of physical time in non-transparent media.

A short list of properties is presented in the following that must be fulfilled by any gaseous, liquid or solid material if it shall be considered transparent to radiation. This applies in particular if transient states have to be analysed.

Assume that a radiation source is placed in front of a non-conducting sample, and that a transmission experiment shall be performed. Close to the sample's rear surface, a radiation detector sensitive to radiation at different wavelengths shall be positioned exactly on the beam axis. If the sample is transparent, and if the detector responds to exclusively the *original* beam (or its residuals, see below), an experimenter will be able to differentiate between

(a) radiation emitted at arbitrary but constant intensity or wavelength, with the radiation source at different positions, or radiation emitted at variable intensity or wavelength, but with the radiation source at a fixed, single position; this includes any position inside the sample volume, and the source may strongly be focussed, like a laser beam, or of extended shape.
(b) monochromatic radiation emitted by source at different intensities
(c) radiation emitted at constant intensity but at different wavelengths
(d) single, isolated pulses or series thereof, or periodic radiation sources, all emitted from any (stationary) position or at any wavelength or at any time or frequency.

In short, if there is a radiation source located within a transparent region of space, and an observer, operating at a position stationary with respect to the source and

within the same transparent region of space, the observer will almost immediately notice any changes of the source's physical properties (position, intensity, wavelength, direction of emitted radiation, stationary or transient behaviour). Limitations are only due to the velocity of light in vacuum.

1.1 Transparency defined by mapping functions

If the observer shall be able to clearly differentiate between corresponding origins and properties of the emitted radiation, it is useful to put the above items (a) to (d) into some mathematical form: Transparency can be described by means of mapping functions, f[e(**s**,t)], that create images of events, e(**s**,t), occurring at locations, s, and at times, t. To uniquely define transparency, the mapping functions must allow creation of images from all events, and allow reverse mapping: The inverse, e(s,t) = f^{-1}f[e(**s**,t)] to f[e(**s**,t)] must exist and uniquely reproduce the underlying events (causes), e(**s**,t). To fulfil these requirements, the mapping functions must be bijective, also allow exchange of positions of sources and observers, at constant distances (or solid angles).

For the mapping functions to be bijective, they must be injective and surjective, in the well known mathematical sense. Assume that there are two events, e($\mathbf{s}_1$,t) and e($\mathbf{s}_2$,t), belonging to a set of events, e(**s**,t), for example emission of radiation at the same intensity and wavelength, from two positions, $\mathbf{s}_1$ and $\mathbf{s}_2$, in space, $\mathbf{R}^3$, and at the same time, t. Another example is scattering of single photons by solid particles with shape, size, electrical conductivity of the scattering centre, and direction of incidence and wavelength identical; scattering like emission shall occur at positions, $\mathbf{s}_1$ and $\mathbf{s}_2$, again at the same time, t.

For the mapping function, f, to be injective, images, f[e(**s**,t)], of all elements, e(**s**,t), of the set must exist. For any pair of elements (events), e($\mathbf{s}_1$,t) and e($\mathbf{s}_2$,t), that occur at the same time, t, but at positions $\mathbf{s}_1 \neq \mathbf{s}_2$, we accordingly request f[e($\mathbf{s}_1$,t)] ≠ f[e($\mathbf{s}_2$,t)], or, if $\mathbf{s}_1 = \mathbf{s}_2$, f[e($\mathbf{s}_1$,t)] = f[e($\mathbf{s}_2$,t)]. The stationary observer shall be equipped with an appropriate detector. Then, in the present case, he recognises, for example, two photons scattered at different positions but at the same time. The photons will arrive at his position at different times of which the difference is given by different lengths of optical paths that the photons have to travel provided their optical paths are located

in regions of space of identical optical properties (no problem in transparent space; relativity effects shall be excluded). The observer would be able to reconstruct the time, t, in transparent space, at which scattering of both photons occurred. The mapping function, for this purpose, has to be injective, in the usual sense: There is *at the most* one image, f[e(**s**,t)], of any of the elements, **e**(s,t), that is created when the mapping function is applied onto elements of this set of events.

In order to conserve transparency in transmission experiments, we have to exclude images of events that do not belong to the set, e(**s**,t), of emissions or scattering interactions; for example, such images might result from noise in the detector or from signals originating from positions outside the considered transparent region of space. In order to exclude such images, the mapping function has to be surjective: All images, f[e(**s**,t)], originate from *at least* one element, e(**s**,t), in the set of events. The mapping function to be surjective accordingly requires that inverse mapping, f^{-1}f[e(**s**,t)], exists for each element of the set f[e(**s**,t)].

In analogy, for any pair of events, e(**s**,t_1) and e(**s**,t_2), that occur at the same positions, s, but at times $t_1 \neq t_2$, the mapping to be bijective requires f[e(**s**,t_1)] ≠ f[e(**s**,t_1)], and the observer recognises both events at different times; here the difference need not necessarily has to be corrected with respect to different lengths of the optical paths.

It is for physical reasons that an additional property has to be defined, which goes beyond usual mathematical definitions of injective and surjective mapping functions:

If two emission or scattering events, e(**s**,t_2)] and e(**s**,t_1), occur at the same position, **s**, in transparent space, and if event (2) occurs only when event (1) is completed, the corresponding images, f[e(**s**,t)], measured appropriately by a clock on a physical time scale, t, shall fulfil f[e(**s**,t_2)] > f[e(**s**,t_1)]. Assume, for example, there are two scattering interactions of a photon occurring at the periphery of a transparent sphere located in an at least partially opaque environment, like a spherical void volume in a solid. A single scattering interaction (2) shall occur only when a preceding interaction (1) is completed. Then, on the physical time scale, t, and as recognised by a stationary observer, the corresponding image f[e(**s**,t_2)] cannot precede the image f[e(**s**,t_1)]. To

be able to recognise the images, the detector would have to be positioned at the radius of the sphere, a situation that might be difficult to be realised.

This additional property of the mapping functions, to conserve transparency, requires the set of images to be ordered. The observer, to recognise this property or perhaps coincidence of events, must be positioned at a stationary place, with respect to the events.

Properties like injective and surjective can be applied to any set, not necessarily to only mathematical sets. Accordingly, the definition of the mapping function, f[e(**s**,t)], applies to all items (a) to (d) of the above if we simply replace time by intensity, wavelength, structure of the source (focussed or of extended shape, delivering single, isolated pulses or continuous waves), respectively.

In Sects. 2 to 5 of the paper, it will be shown that mapping functions, f[e(**s**,t)], are not bijective if attempts would be made, in non-transparent media, to describe correlation between events and images.

1.2 Non-transparency

The question comes up: What happens if items (a) to (d) of Subsect. 1.1 would *not* be fulfilled? Optical thickness indicates the total number of mean free paths when a photon travels through a sample.[1] A sample is transparent if its optical thickness, τ, at all wavelengths is zero (or at least extremely small, an ideal situation approximately fulfilled in some dilute gases). If the optical thickness is zero, the photon will not be scattered into directions different from the original beam, and there is also no absorption/remission. The case $\tau = 0$ accordingly indicates direct transmission. If τ is not zero, the residual intensity observed by the detector is given by application of Beer's law provided the detector again responds to solely radiation transmitted exactly in the beam axis.

But strong forward scattering may redirect extinguished (previously scattered or absorbed/remitted) radiation to the original direction. This is fulfilled, for example, if the wavelength of incoming radiation is small in relation to the dimension of the

scattering object. Even if the medium has only backward-scattering but no absorption/remission properties, this contribution will not be negligible. Accordingly, if the detector sees some radiation, this not necessarily indicates transparency.[2] Even if $\tau >> 0$, the medium though non-transparent could be translucent, like a thick fog that in all directions uniformly screens direct solar radiation incidence. For the medium to be almost completely non-transparent, a simple estimate shows that it is (with some generosity) sufficient to have an optical thickness of at least $\tau = 15$, because in this case the ratio of residual to original intensity according to Beer's law is below 10^{-6}, a number small enough to say there is almost no directly transmitted radiation from the source. If $\tau \rightarrow \infty$, a non -transparent medium finally acts like a heavy, opaque curtain.

Looking through opaque curtains onto structures or processes behind is impossible even if the curtain would be constituted by only an extremely thin, non-transparent film (its extinction coefficient then would have to be very large). But is it possible to analyse processes proceeding in the *interior* of a non-transparent medium? The answer that presently can be given is: Space horizons of observers operating in front of a non-transparent curtain simply terminate at this structure.

Non-transparent media, if not only interpreted from standard radiative transfer standpoints but also considering propagation of excitations other than by photons (for example elementary or even solid particles), cover the vast range between thin (at least 100 nm thickness) metallic films, packed or fluidised beds, solids like metals and superconductors, thermal insulations, chemical and nuclear reactors (the moderator), the Earth's crust, the atmosphere of the Venice, mostly in the infrared wavelength regions, the outer layers of the Sun, and even dark clouds and other very large cosmological objects, these at least at visible wavelengths, while infrared radiation from regions behind such curtains, like radiation from young, bright stars, can well be detected.

---

[1] In a real sample, length of mean free path and thus optical thickness, the total number of mean free paths, both are statistical quantities.

[2] If this radiation is of a wavelength different from the wavelength of the original source, differentiation between original (i. e. the residual) and remitted radiation might be possible.

Fig. 1 shows a schematic division of non-transparent media against their transparent or translucent counterparts.[3] The figure also localises dispersed media: solid, liquid or gaseous substances that are dispersed with respect to radiative transfer. Dispersed media are so finely divided and insolubly distributed in vacuum or in a different hosting solid, liquid or gaseous medium that they are in a considerably higher state of energy than their proper compact phase. For the radiative case, it is sufficient that the constituents of the dispersed medium have a refractive index different from the index of the hosting environment. Non-transparent media in many cases are highly dispersed.

Any non-transparent curtain divides space into regions of completely different properties of radiative transfer. This applies to all laboratory or technical objects regardless of their size.[4] Such divisions might be manifested by sharply defined planes, or instead, by diffuse boundaries. Particle beds and dark clouds or other very large, non-transparent objects usually do not have sharply defined “radiative” surfaces but diffuse boundaries. The thickness of the diffuse region depends on the mean free path, strictly speaking on multiples thereof, of photons; they could be emitted or forward scattered not only from exactly the surface but also from internal regions of these curtains and by transport processes directed onto an observer operating in transparent space outside the curtain. The same consideration in principle applies to also scattering and emission of quanta or particles other than photons.

In non-transparent media, radiation propagation can be described as a diffusion process (radiative transfer in such media has frequently been studied in the literature, for a survey see the literature cited, for example, in Refs. 1 – 3). As a consequence, also residual radiation seen by a detector located near the rear surface of a non-transparent sample will be diffusely distributed. Then, from measurement of solely the intensity of residual radiation, it is neither possible to safely make decisions concerning the properties of the radiation source nor the internal scattering and absorption/remission properties even if the radiation source would strongly be

[3] In this paper, non-transparency and opacity will be used as synonyms; non-transparent media may be considered also as opaque “curtains” for a real observer positioned in front of such a curtain.
[4] This applies also to formal descriptions of the present structure of the universe that rely on a division of transparent regions of space (the well-known spherical space-time geometry) and an opaque enclosure (a hot background located behind the most distant, presently known objects).

focussed in the direction of the detector or if the scattering properties of the medium are highly anisotropic (illustrative examples are given in Sect. 5 and in Appendices A1 and A3).

So far, all this is well known. In this paper, we will go a step ahead. While space horizons have extensively been treated in highly qualified standard textbooks (see e. g. Ref. 4) and in a large variety of individual papers, the second item, *time* horizons, apparently has received less attention. This is the subject of the present paper.

Any event like emission of a beam or of only a single photon, at a time t_0, into a transparent sample is definitely correlated with the (physical) time, t_1, at which a detector responds to this event. The detector's response at this time allows to uniquely identify the event "emission of a beam or of particles" *if* it is located in a *transparent* medium (this is simply a time-of-flight experiment). Does this correlation exist also in case such events take place in a *non-transparent* medium when direct observation of events (emission from a source, scattering) is not possible?

The paper is organised as follows: In the remainder of Sect. 1, we summarise usually accepted properties of physical time and its contrast, psychological time, as far as application to non-transparent media would be concerned. This discussion serves to prepare Sects. 2 to 6 where real and virtual observers, operating in front of or inside a non-transparent medium, are introduced to precisely define the central problems of this paper: Does physical time exist in non-transparent media? If it would exist, to which extent can physical time then be ordered? These questions are also related to a temporal cloaking experiment very recently reported in the literature, and serves to discuss in Sect. 3 the possible existence of time holes under the conditions transparency or non-transparency. Sect. 4 considers entropy production in non-transparent media, to support the conclusions made in the preceding Sections. Numerical examples for propagation of radiative pulses, like in laser-flash experiments, and of excitations other than radiative are presented in Sect. 5 and in the Appendices, to further outline the central problem: Is it possible to correlate events by means of physical time scales inside and outside a non-transparent medium? At the end of the paper (Sect. 6), invariably the question comes up, and is indeed tempting to discuss, whether the demonstrated limitations to existence and

order of physical time would have any consequences for research in objects of much larger than laboratory dimensions, for example into the past of the universe. Sect. 7 summarises limitations to existence of physical time, coincidence and correlations.

1.3 Properties of physical and psychological time

As commonly accepted, physical time in a mathematical sense may be identified with the set, R, of real numbers (see, for example, Ref. 5). The set R is totally ordered: If a_1 and a_2 are elements of R, then one and only one of the following three relations holds: $a_1 < a_2$, $a_1 = a_2$ or $a_1 > a_2$. The set R also is dense, a continuum. Under this assumption (i. e. physical time identified with R), physical time in classical mechanics and in other classical disciplines allows representation of the corresponding laws of physics as differential equations, with respect to time. Classical mechanics in otherwise empty space, and without disturbances, is invariant under reversal of physical time; trajectories would not change when projected into past or future if observers do not move relative to the objects. The same applies to Fourier's differential equation: It is linear in time otherwise transformation of time, t, to its negative, –t, would allow heat flow from regimes of low to high temperature (or of matter from regions of small to regions of high concentrations), clearly impossible. As Prigogine and Stengers (Ref. 6) pointed out, physical time is considered reversible also in relativity.

An asymmetry of the direction of physical time, and thus an orientation of the arrow of time, becomes probable when the 2^{nd} law of thermodynamics is taken into account. Mathematically, irreversibility then reduces R to the half-set R^+. Hund (Ref. 7), when referring to the work of Lemaitre, said a distinction between past and future relies on a very improbable, initial, minimum entropy state of the universe, which means the universe, after an initial (zero-) point of space and time, could develop solely into a single direction of physical time.

Whether the arrow of physical time, in contrast to its psychological counterpart, can be extended indefinitely into the future will not be discussed here. The other extreme, a lower limit of (successive) time intervals, when physical time no longer must be considered a continuum, is given by the Planck time, $t_P = (h\ G/c^5)^{1/2}$, about 10^{-43} s, with h and G the Planck and gravitation constants, respectively, and c the velocity of

light in vacuum. Planck time, t_P, *per definition* indicates the minimum, non-zero physical time interval that light needs to travel across the Planck length, about 10^{-35} m. The Planck length determines a lower limit up to which standard physical theories are applicable. For the moment, Planck time can be neglected: Time steps between successive interactions of radiation with ordinary dispersed materials, or even between collisions of nuclei in an excited nucleus, are larger, by many orders of magnitude, than t_P.

Time, physical or psychological, cannot be imagined without events; we will later (Sect. 2) have to check whether this statement is valid in both directions. Physical time, or direction of its arrow, must closely be related to many-particle systems that experience a large number of interactions (events) when developing into a single direction of time. Physical time accordingly does not exist a priory, neither without space nor without a multiple of events (in many-particle systems). Accordingly, consideration of physical time has to involve many-particle systems and their states.[5]

In the following, we will indicate when these commonly accepted properties of physical and psychological time would require special attention if non-transparent media have to be considered.

Assume that two scattering and absorption/remission events, e_1 and e_2, are observed at positions x_1 and x_2, respectively, with $x_2 > x_1$ (in any coordinate system) measured on the complicated path that a single photon travels through a non-transparent medium. Because of the 2nd law of thermodynamics, the corresponding physical arrival times, t_1 and t_2, of the photon at these positions (or the times when interactions occur at these positions), respectively, are ordered. We accordingly have $t_2 > t_1$ while the relations $t_2 = t_1$ or $t_2 < t_1$ are forbidden because these would be in contradiction to the total order of the set R^+ provided physical time may be identified

[5] Physical time came into being only after an initial singularity developed into events (expansion of space, condensation of energy to radiation and matter). The idea of a singularity from which physical time is created (and is extending in only one orientation) is indeed relevant predominantly in cosmology. It is supported by variety of observations or theories like the presently observed very smooth distribution of 2.7 K-background radiation, experimental confirmations of modelled light element (He, D)-abundance, the solutions of Einstein's equations and by Hund's initial (thermodynamic) state. Hawking and Penrose demonstrated that any model of the universe based on approximate homogeneity and isotropy, as is apparently realised, must start from a singularity (see, for example, the discussion in Ref. 8, Chap. 9). But the problem of definition or identification of a zero-

with this set in non-transparent media. Without this restriction, it appears physical time when related to events also in non-transparent media should be monotonously ordered (again, we will have to discuss this property in Sect. 2).

Both physical time, as a measurable quantity and located within the half-set R^+, and psychological time, as experienced (or simply imagined?) by human beings, allows arbitrarily large numbers of events: There is neither a maximum number of events in non-transparent media nor exists a maximum element in R^+. But only physical time defines a point-wise, *sharply* defined „presence“, or even an arbitrary series of presences, and thus separates on its scales a corresponding arbitrarily large number of „pasts“ and „futures“ from each other. In Sect. 2, it will be discussed whether this view is valid also in non-transparent media.

Instead, psychological time considers only *one* single presence that has a very specific property: A time *interva*l of non-zero length, perhaps a few seconds measured on physical time scale; the actual length of presence is subject to each individual. Psychological time, unlike physical time, cannot without contradictions (Zenon’s paradox) imagine a zero length event, or sequences thereof.

Physical time *does* allow zero length elements, for example if the events e_1 and e_2 observed on the path of the (single) photon in a non-transparent medium coincide at the stationary x_1 and x_2 which implies the difference $t_2 - t_1$ of arrival times should be zero (or the length of a corresponding vector be zero, the zero element of a vector space to be defined in Subsect. 2.1).

Like physical time, psychological time is a causally ordered sequence of events, but all of *finite* length, contrary to physical time. Psychological time yet is not an algebraic sum of measurable, non-zero length intervals. Psychological time, in our imagination, extends in *both* orientations to infinity. Both orientations emerge from a (finite) presence interval.

Properties like these (extension of time in *both* orientations to infinity) cannot be realised with physical time. Instead, an *initial*, sharply defined presence, e. g. a

point of physical time comes up also when investigating transient states in objects of modest, much

singularity, as the zero-point of physical time scales defined independently for each real observer, either is postulated to conserve causality (or to avoid problems arising from negative times), or it is deduced from experimental or theoretical results using appropriate models for description and analysis of past and future (an open question is whether these models *a priori* incorporate, or are based on, the idea of a singularity). The question to be discussed in Sect. 2 is whether a zero-point of physical time scales can be postulated or deduced also with respect to events in non-transparent media.

Since physical time is monotonously ordered, this means that at least the origin of physical time could rely on a property of psychological time (causality) while the idea of a *zero-point* cannot be deduced from, and instead is a contradiction to, psychological time. Psychological time neither can accept „points“, i. e. events of zero length like a zero-point of time, without running intro contradictions, nor could it accept an arrow of time oriented into a single orientation only.

If we return to Planck time: Also the question comes up whether physical time, or corresponding time-like sequences of images in non-transparent media (Sect. 2), could be identified with a large multiple of Planck times.

In summary, definition of the arrow of physical time apparently has profited from at least two properties of psychological time:

(i) part of the „infinity property“ of psychological time (infinite in one orientation, a property that possibly could be valid only temporarily),
(ii) a monotonously increasing, causal order. Yet physical time is not identical to psychological time. Physical time has no memory.

Physical time cannot exist without events. What are “events”? In this paper, we are mainly concerned with radiative transfer. Events then are understood as interruptions of the paths that photons travel, by scattering and absorption/remission interactions with matter. In a non-transparent medium, the number of interruptions is very large. If we assume a cloud of photons emitted from a source, propagation *of the cloud*

---

smaller dimensions.

through the medium can be correlated with physical time of events that it initiates, certainly on a statistical basis only. Provided fast detectors are available, this measurement can be realised inside or outside the corresponding medium.

Positions of the wave front can also theoretically be indicated, as a function of time, if the propagation velocity is known. We have to differentiate a purely scattering from an absorbing medium. In the first case, it is the speed of light, in the second the propagation velocity is given by an expression containing the thermal diffusivity of a (conductive) material (Sect. 5, Appendices). Thus positions, x, of the cloud on its way through the sample can be assigned arrival times, t(x): For x' > x, we have t(x') > t(x), the monotonous order, regardless whether the medium is only scattering or absorbs and emits radiation. But a difficulty arises from the observation that each individual photon of the cloud travels its *own* path regardless of the propagation of its companions (with exceptions from quantum correlations not considered here; it is indeed the question whether quantum entanglement would operate in non-transparent media). All these paths are only statistically defined, and thus are independent of each other. This means the arrival times of each individual photon, for example at planes x located parallel to the sample's surface, cannot be identical, it is a distribution (a "cloud") of arrival times that is observed.

Based on these preliminary considerations of transparency and physical vs. psychological time, we will demonstrate in the Sects. 2 to 5 that neither

(a) existence of physical time, as a dense set of uncountably infinite elements,
(b) uniquely defined monotonous order of physical time nor
(c) existence of a zero-point of physical time, uniquely defined only after a singularity

can rigorously be deduced and confirmed by observers if they operate in front of, or inside, a *non-transparent* medium. If these observers postulate an origin of time, a conclusion like this cannot stem from own experimental findings but rather might be a result adopted from psychological time.

1.4 Two extreme cases: radiative exchange, radiative transfer

Assume two real observers positioned at different locations in otherwise empty space. The first observer shall report a series of events that on his physical time scale either are coincident or monotonously ordered. The second (real) observer will report coincidence, or the same monotonous order of events, respectively, provided the following conditions are fulfilled:

(i) the second observer does not move relative to the first,
(ii) there are no „obstacles“ located between positions of the observers and the locations where the events take place; such obstacles could interrupt, deteriorate, delay and even completely suspend exchange of information. The exchange may be realised by emission and detection of light signals or other carriers of information,
(iii) both observers operate in the *same* environment (no obstacles).

This is radiation *exchange*, *one* of the two extreme cases of radiative flow: Absolute transparency, direct transmission, propagation of light through empty space. We will in the present paper not consider curved space-time and phenomena like gravitational lenses and their possible impact, if any, on transparency or its complement. The other extreme case is radiative *transfer* in a non-transparent medium.

2 Mapping functions

2.1 Modelling physical time as a 1D vector space

Physical time, t, frequently has been added to the usually considered 3-dimensional Euclidean space (x_k, $1 \le k \le 3$) as a 4^{th} independent component ($x_4 = i\,ct$, with c the speed of light). Such 4-dimensional construction neither appears to be very descriptive (compare the comments in Ref. 9) nor is it obvious that the coordinate x_4 can be assigned a spatial quality.[6] At the end of Subsect. 2.3, we will see that treating physical time as the 4^{th} component of a *common* 4-dimensional vector space *in non-transparent media* invariably would lead to contradictions. We will instead construct the arrow of physical time in a separate vector space, to allow analysis of this very space independently of properties of the space $\mathbf{R}^3$. This does *not* introduce

new physics, it is used only as a tool to facilitate the following discussion, rather in a didactic sense (it will become clear that it is indeed a key to improve understanding of physical time in regions of space that have strongly differing optical thickness).

As usual, points in the Euclidean space $\mathbf{R^3}$ shall be interpreted as endpoints of vectors constructed from multiples and linear combinations of basic vectors $\mathbf{r_k}$ ($1 \leq k \leq 3$). The symbols, $\mathbf{r_k}$, are taken to indicate basic vectors of this space, instead of the usually applied symbols $\mathbf{e}_k$, to omit confusion with events, e(**s**,t). Bold symbols like **s** denotes vectors.

By analogy, we will assume physical time occupies a separate, independent vector space, **Z**, which is constructed from basic vectors $\mathbf{z_i}$. Vectors in **Z** are created when a clock coupled to an experiment performed in $\mathbf{R^3}$ indicates that an "event" has taken place, and the physical time noted at this instant gives the length of the corresponding vectors in **Z**. Experience with psychological time suggests **Z** is one-dimensional, $\mathbf{Z} = \mathbf{Z^1}$.

In *transparent media*, both vector spaces $\mathbf{R^3}$ and $\mathbf{Z^1}$ are correlated in the following sense: All vectors in $\mathbf{Z^1}$ in the following are obtained from application of uniquely defined mapping functions that couple events in the completely transparent $\mathbf{R^3}$ with elements of $\mathbf{Z^1}$ (whether the vector space $\mathbf{Z^1}$, too, might be considered as "transparent" will be discussed in Subsect. 3.3). Before, it has to be decided whether a mapping like this can be realised at all also in case of non-transparency, and if it exists, whether this mapping could uniquely be defined.

Assume, for example, that a particle moves in the completely transparent (empty) $\mathbf{R^3}$, with a velocity $v << c$, from the zero-point of a co-ordinate system to an end-point, $\mathbf{s}_1$. We define a mapping function $f(\mathbf{s}_1)$ that assigns the point s_1 in $\mathbf{R^3}$ exactly one point t_1 in $\mathbf{Z^1}$: $t_1 = f(\mathbf{s}_1) = \alpha\, \mathbf{z_1}$ (Fig. 2), with $\alpha \in R^+$.

We will not discuss whether all requirements are fulfilled to correctly assign the physical time space $\mathbf{Z^1}$ the quality of a vector space (psychological time certainly would not fulfil vector space axioms). A zero-element of physical time has to be

[6] Nevertheless, coordinates x_i ($1 \leq i \leq 4$), as is well known, allow an elegant, 4 x 4 matrix derivation of

postulated (to fulfil the property mentioned in Sect. 1.3), otherwise it would not be possible to define coincidence in $\mathbf{Z^1}$, and confusions between physical and psychological time would be the consequence. The mathematical structure of $\mathbf{Z^1}$ is close to the theory of one-parameter half-groups (Ref. 10).[7]

2.2 Mapping events from $\mathbf{R^3}$ to $\mathbf{Z^1}$

Assume next that a *non-transparent* medium, for example a disk of finite thickness D, partly fills $\mathbf{R^3}$ (Fig. 3). Its optical thickness, τ, shall be very large but finite (the extinction properties accordingly are finite, too). A source Q located outside the non-transparent medium emits radiation pulses (of Dirac type, or of finite length) to the front surface of the disk; the pulses shall impinge under right angles onto the surface (this assumption does not lead to loss of generality; it is made only to simplify the discussion). Because of the large optical thickness, a photon initially absorbed at, and then remitted from, the front surface (x = 0) will have to travel a very large number of steps (mean free paths) between front and rear sample surface. We assign an "event", e(**s**,t), to each scattering or absorption/remission interaction during this period of time.

We further assume that a real observer is located at a position **A** outside the non-transparent disk (but within $\mathbf{R^3}$). However, since this observer cannot control what happens inside the non-transparent sample, we need another, a *virtual* observer to support him, who recognises all internal events and indeed shall be able to supervise the whole trajectory of the particle inside the non-transparent region (a real observer, any imaginable detector, could hardly do so). Assume that the virtual observer operates at an arbitrary position **B**, with x-coordinates 0 < x < D in the non-transparent region (like the position **A**, the position **B** need not be specified explicitly with respect to coordinates y and z).

2.2.1 Comparison of observations external/internal to non-transparent space

First some specifications to the real observer: Positioned at or near the rear side of a non-transparent region of space, he recognises solely isotropic distributed radiation intensity. Since he does not know anything about the radiation source, he even does

---

relativity principles.

not know this is the residual intensity of a pulse emitted from a source (or from a target spot at x = 0 where the emitted radiation is absorbed first and remitted). For example, he instead could assume the intensity distribution that he observes results from another radiation source located behind him and is the result of diffuse reflection from the rear sample surface (in front ob him). Further, the real observer neither shall know geometrical nor optical thickness of the slab nor shall he know scattering and absorption/remission properties of the sample material between x = 0 and x = D.

Assume provisionally that a physical time scale, t, exists also within the non-transparent region. We will very soon understand that this assumption cannot be realised with conventional time scales, but let for the present discussion the virtual observer be furnished with a clock that on this (pseudo-) physical time scale "books" images, f[e(**s**,t)] = t, of all internal events e(**s**,t), for example those occurring at positions s_1 and s_2 that a photon travels on path W_1 in Fig. 3. The virtual observer recognises these events on his (and solely on his) time scale, t. The real observer instead does not know anything about events at these positions and, in particular, he does not know anything about time scales within this region. He may only *believe* that time scales inside the non-transparent region might exist and, if so, should be identical to his time scale.

The virtual observer might attempt to approach positions $\mathbf{s}_1$ or $\mathbf{s}_2$ as close as possible, in order to resolve the distance between images f[e(**s**,t)] of events occurring at $\mathbf{s}_1$ and $\mathbf{s}_2$ on his time scale, t, into arbitrarily small time steps. However, this is not possible without limitations, for two reasons:

a) Distances between $\mathbf{s}_1$ and $\mathbf{s}_2$ smaller than the mean free path, l_m, of a photon cannot be detected because the lower limit of these distances is given, on the average, by just one mean free path along path W_1, and no further scattering or absorption/remission as the immediately next event at $\mathbf{s}_2$ following $\mathbf{s}_1$ will occur in-between

[7] Although zero length intervals do not exist in psychological time, this does not exclude coincidence: it is simply the identity of images on psychological time scales, which is not the same as a zero length-difference between two images on physical time scales.

b) propagation of information is limited by the time needed to transfer the information (the images) obtained at $\mathbf{s}_1$ and $\mathbf{s}_2$ to *his* position, **B**; this is at least the time that a photon needs to travel the distance l_m.

Assigning to also the real observer a clock means that this observer will book images, too, but of quite different properties. In his case, an image is given, for example, by the time, t', at which a temperature excursion, T(x,t), at the rear surface (x = D), i. e. a macroscopic physical quantity, attains a certain value, T(x=D,t'). The real observer *believes* this is the result of, and definitely coupled with, a very large number of internal scattering and absorption/remission events, e(**s**,t), the impact of the travelling single or of a cloud of scattered and absorbed/remitted photons. In logical sense (cause precedes effect), these interactions are indeed the cause (at least partially, because there might be also conduction) for the observed temperature excursion, T(x=D,t'). However, if the medium is non-conducting, he does not know whether it is a *single* photon or a *cloud* of photons each travelling through the sample on an internal physical time scale, t, that causes the temperature excursion observed at his physical time, t'. Though detection, by means of a temperature measurement, of the impact arising from absorption of just a single photon would cause him great experimental difficulties, we can assume, provisionally and only for the present discussion, that he could be successful.

When the experiment is completed (all photons initially emitted by the source, Q, or, respectively, the photons remaining after a multiple of scattering and absorption/remission events) have left the sample, the virtual observer shall be allowed to report the final result (solely the detected elements of $\mathbf{Z}^1$) to the real observer, just for comparison of the time scales, t and t', and for control what the real observer has believed until this moment. It is of little importance how the virtual observer would realise "reporting" (certainly not by photons, as these would also be scattered or absorbed/remitted). It is only to enable the real observer to compare what the virtual observer recognised on his private time scale that now is projected on *his* (the real observer's) external scale, t' (instead of the activity "reporting", we could simply say the events e(**s**,t) occur at times f[e(**s**,t)] = t, regardless whether a real observer recognises the events or not).

The real observer,

(a) if he observes radiation signals only: recognises at the sample's rear surface, x = D, a completely diffuse distribution of intensities, i'(x=D,t'),
(b) if he observes temperature signals only: recognises a temperature variation, T(x=D,t'), at the same position. Frequently, temperature measurement at the sample's rear surface is realised by means of a radiation detector.

In case (b), from the imagination that temperature fields must be differentiable with respect to space coordinates (no temperature jumps in a conducting sample), and time, he can only *believe* using corresponding analytical models, i. e. on purely theoretical grounds, that there should be clearly defined temperature excursions not only on the sample's rear surface but also within the non-transparent sample if it has conduction properties. In this case, he will be in a position to indicate quantitatively the excursion $T(0 \leq x < D,t')$ at *any* position, x, if he applies T(x=D,t') as a boundary condition.

In case (a), however, he cannot apply a boundary condition i'(x=D,t'), to quantitatively describe the inner radiation field, $i'(0 \leq x < D,t')$, at *any* position because intensity at these positions is only statistically defined (only in the limit $\tau \rightarrow \infty$ will it be possible to assign radiative transfer a conduction-like behaviour). Beer's law could be applied only in particular directions within the medium since it describes *residual* intensities, not a distribution of residual intensities (after scattering and absorption/remission, i. e. extinction interactions) plus intensities redistributed to this particular direction; this is the (difficult) task of the general equation of transfer.

While in case (b), correlation between time, t', and temperature field, T(x,t'), would be unique, since the prediction can be based on application of Fourier's differential equation, this is not fulfilled in case (a) where the statistical distribution of the intensities could only be approximated (if $\tau \rightarrow \infty$) by an analytical and differentiable expression.

In both cases, the real observer further has to *believe* both time scales, t and t', would exist and be identical. Even if this were fulfilled, the real observer, from the

images, t', will not be able to uniquely correlate these images with images, t, that the virtual observer booked in his space, $\mathbf{Z}^1$: Corresponding mapping functions neither are injective nor surjective:

To be injective, a time scale, t, at which radiative interactions occurred, at a position x within the sample, as reported by the *virtual* observer, would have to be correlated uniquely to a time scale, t', at which local temperature, T(x,t'), at or near the same position (within the distance, l_m) observed by the *real* observer, would attain a specific value, clearly impossible. The real observer cannot detect temperatures neither at this internal nor at any other position within the sample (with the exception of a diffuse layer of maximum thickness l_m near the sample's rear surface). He can only *believe* in the existence of the excursion, T(x,t'), on the basis of analytical models.

To be surjective, time t' at which T(x,t') attains a specific value, should result from at least one event within the sample that occurred at a time, t. The excursion T(x,t') certainly relies on a very large number of scattering plus absorption/remission events, but not necessarily on events booked on the time scale, t, of the virtual observer even if the real observer could resolve temperature variations that might follow absorption of just a single photon. This absorption event occurs at positions $0 < x < D$, i. e. least at a distance l_m from $x = D$. Because of the finite value of the speed of light, the corresponding images, t and t', cannot be identical. Thus, in non-transparent media, mapping functions are not bijective.

So far we have implicitly assumed existence of a time scale, t, on which the virtual observer books his observations (this is the assumption provisionally made at the beginning of this Section). Accordingly, the question comes up whether this assumption can be confirmed. For this purpose, the discussion cannot be confined solely to comparison of images, t', on a time scale outside the non-transparent sample, with events booked on a time scale, t, within the same sample. The very existence of the internal time scale, t, itself has to be questioned, on a basis exclusively prescribed by the properties of R^+. The corresponding discussion is given in Sect. 2.3; it will be prepared in the next Subsection.

2.2.2 Comparison of observations all within non-transparent space

The total length, S_R, that photons have to travel along the schematically indicated, dotted paths, W_1 or W_2, in Fig. 3, between the planes x = 0 and x = D in $\mathbf{R^3}$ and as seen by the virtual observer at position **B**, is given by the algebraic sum $S_R = \Sigma\ \xi_k$ taken over N corresponding mean free paths ξ_k ($k \leq N = \tau$). It is clear that $S_R \geq D$, because of the large τ (the larger τ, the more will $S_R >> D$ be fulfilled, on a statistical basis).

Each scattering or absorption/remission event as booked by the virtual observer when the photon arrives at the corresponding end points $\mathbf{s}_k$ of the individual steps, i. e. the sum $\Sigma\ \xi_k$ over the single mean free paths, ξ_k, is assigned a corresponding vector (the image) in $\mathbf{Z^1}$. This means if events $e(\xi_k)$ are monotonously ordered with respect to distance from the origin seen along a path W, with $\mathbf{s}_1 = \xi_1 < \mathbf{s}_2 = \xi_1 + \xi_2 < \mathbf{s}_3 = \xi_1 + \xi_2 + \xi_3 < \ldots < \mathbf{s}_N = \Sigma\ \xi_k$, their images $f(\xi_1) = t_1$, $f(\xi_1 + \xi_2) = t_1 + t_2$, $f(\xi_1 + \xi_2 + \xi_3) = t_1 + t_2 + t_3$,...,$f(\Sigma\ \xi_k) = t_N$, are monotonously ordered as $t_1 < t_1 + t_2 < t_1 + t_2 + t_3 < \ldots < t_N$; this is a logical consequence.

If E denotes the extinction coefficient of a bed of solid particles, and if, for example, $E = 3.3\ 10^4$ 1/m, the mean free path, ξ, amounts to about 30 µm. This means the minimum distance, Δt, between end points of vectors in $\mathbf{Z^1}$ with images that result from events occurring in space on the *same* path, W, and that are separated by at least the step $\Delta s = \xi$, is about 10^{-13} s, as notified by the virtual observer (using the speed, c, of light of the photon and for simplicity assuming an index of refraction n = 1 of the bed). The minimum distance, Δt, of images under this condition, is not zero, contrary to what is required if the commonly accepted property of the half-set R^+ holds (we could assume also events created by propagation of particles other than photons).

This is a first indication that proof of existence of physical time in non-transparent media might become difficult. We will see in the following that it is easier to prove *non-existence* of physical time, and this will be done in three steps:

(i) the general validity of the theorem “no time without space and events” is accepted

(ii) images f[e(**s**,t)] do not constitute a dense set if they are created by application of mapping functions, f, on events e(**s**,t) occurring in non-transparent space

(iii) sets of images do not create physical time but only time-like sequences if the images are not uncountably infinite.

Item (i) besides relativity principles also reflects existence of time holes. In a time hole (a certain "empty" time interval), the time axis, considered as a collection of images of events, does not contain images. The statement "no events, no time", if taken from left to right, means: If there are no events that could have occurred within a non-zero interval of physical time, accordingly there can be no images of events (times) that could be detected during this period. While this sounds trivial, it is correct only if for any event there is at least one image. The question is whether this statement is also correct if considered in the opposite direction: If there are no images, accordingly are there also no events that could be assigned a definite time when they occurred? We will come back to this question in Subsect. 3.2.

2.3 Theorems proving non-existence of physical time in non-transparent space

Even if a real observer could enter the interior of a non-transparent slab, he would recognise nothing but diffusely distributed radiation, probably of increased intensity the more he approaches the radiation source, as long as regions of large optical thickness like in Fig. 3 are between the source and his position. If the optical thickness of the sample increases without limitation, $\tau \to \infty$, the real observer like his virtual colleague, could try to overcome this problem by approaching the source (the target spot) as arbitrarily close as possible. Even then would he not recognise anything else than isotropic radiation intensity (provided there is indeed any intensity left when gradually $\tau \to \infty$). He also would not recognise anything else but infinitesimal small *yet non-zero*, minimum differences, Δt, between endpoints of vectors in $\mathbf{Z}^1$. Propagation of radiation in $\mathbf{R}^3$, under these conditions, cannot be described as a dense series of events and, accordingly, cannot constitute as well a dense series of images in $\mathbf{Z}^1$, a contradiction (in non-transparent space) to the commonly accepted assumption that physical time is dense like the elements of R^+.

If events belong to exactly the *same* physical experiment, all physical events and their images, both among themselves, can uniquely be distinguished: Events are different in $\mathbf{R^3}$, for example, if either propagation of an object from one coordinate to another is considered. This also applies to images in $\mathbf{Z^1}$ if successive events simply are repetitions occurring at the same positions in space.

We may argue there might be also events other than created by propagation of radiation, like propagation of phonons in a crystal lattice, diffusion of chemical species under concentration gradients, phase transitions, decay of radioactive impurities, to mention only a few. All images resulting from these events are booked, now by corresponding virtual observers that have appropriate mapping functions available, to create images in $\mathbf{Z}^1$. But it is not possible to fabricate in this way a dense series of images, as elements in $\mathbf{Z^1}$ or in other images spaces.

All these conclusions will now be condensed in the following two theorems.

Theorem 1: With non-transparent media, it is not possible, by means of mapping functions, f, to create a dense set of elements in an image space that is contained in the half-set R^+ of real numbers,

(i) if the functions f apply as their arguments the coordinates of *physical events* located in any event space, and

(ii) if the coordinates of the events are uniquely defined by endpoints of vectors **s** that are multiples $\mathbf{s} = \beta_k\, r_k$ or linear combinations $\mathbf{s} = \Sigma\, \beta_k\, \mathbf{r_k}$ ($\beta_k \in R^+$, $k \leq 3$) of basic vectors, $\mathbf{r_k}$, of a set $\mathbf{R^k}$, and

(iii) if the set $\mathbf{R_k}$ is identical to or contained in ($k < 3$) the usual vector space $\mathbf{R^3}$, and

(iv) if the events belong to the same physical experiment, and

(v) if the mapping functions, f, are continuous, and

(vi) if the images f[**s**(e)] are elements of a common, single image space

(vii) if the image space is stationary

To give an example to item (iv), the same physical experiment in case of radiation propagation is given by a path, W', in the medium though, during the period of time a beam travels through the medium, secondary beams or photons can be emitted, after

corresponding absorption/remission interactions, that then travel on paths W'' usually different from W'. Only if the medium is solely scattering will the path W' be conserved: *One* beam or one photon means exactly *one* though complicated path (photon or another carrier shall not be split into sub-particles if the non-transparent medium is solely scattering).

Proof of theorem 1

Assume two arbitrary but different events, e_1, e_2, the coordinates of which are given by corresponding vectors $\mathbf{s}_1$, $\mathbf{s}_2$ located in the same event space. Distance, $\Delta\mathbf{s}$, of the coordinates is given by the difference $\Delta\mathbf{s} = \mathbf{s}_2 - \mathbf{s}_1$ (in $\mathbf{R^3}$ or in any of its subsets, $\mathbf{R}^k$) between events not only belonging to the same physical experiment (item iv) but also occurring under the same physical (initial or boundary) conditions; all other conditions as defined above by items (i) to (vii).

The difference $\Delta\mathbf{s}$ in non-transparent space never becomes zero. Since it was defined (condition vii) that the image space is stationary in relation to the event space, which means any observer does not move relative to the events, no transformation of positions or times, individually experienced by an observer, that could be requested from relativity principles, is necessary. Accordingly, assume that there are two events, e_1, e_2, with e_2 occurring not before e_1 has been completed. If then in this set the relation $\mathbf{s}_1(e_1) \neq \mathbf{s}_2(e_2)$ holds, their images f[**s**(e)] created by any continuous (injective) mapping function, f, are not identical, f[**s**(e)] ≠ f[**s**(e)], in any image space (not necessarily sets R^+ or spaces, $\mathbf{Z^1}$; we neglect a possible impact of quantum entanglement). Accordingly, if any set **S** of coordinates **s** of events (of arbitrary large number) is contained in an event space $\mathbf{R^k} \in \mathbf{R^3}$ ($k \leq 3$), $\mathbf{R^k}$ being a subset of $\mathbf{R^3}$, and if the elements of this set, under the above items (i) to (viii), would not constitute a dense set (because the difference $\Delta\mathbf{s}$ under physical conditions cannot become zero), then the corresponding set of images, f[**s**(e)], in any image space, for example in $\mathbf{Z^1}$, too, is not dense. This conclusion simply relies on the property of any continuous mapping functions defined on elements of R or R^+ (here with the expansion coefficients $\beta_k \in R^+$ or any of its dense and ordered subsets).

End of proof

Now let events and their images result from *more* than one physical experiment, for example radiation propagation in parallel to thermal conduction heat flow or if the sample is unstable to nuclear decay. In this way, a set of image sets, J, will be fabricated, and the images resulting from different physical experiments are to be collected on a single, common time scale, by appropriate injective mapping functions. We can tentatively assume that the number of different physical experiments (like propagation of radiation, decay of radioactive species, all within the same medium) could be increased strongly (which in reality is hardly possible), or that the number of initial or boundary conditions or in particular of optical properties in a limited number of physical experiments would be very large. The latter condition can be approached, for example, by increasing, in a specific radiation transfer experiment, the optical thickness gradually to $\tau \rightarrow \infty$. This generates a set of different experiments because for any optical thickness, there will be a different number of paths with a different distribution of scattering, absorption/remission events on each path. But the number of such experiments (the number N of elements of a corresponding set M of experiments), though potentially very large, neither is uncountably infinite nor is it infinitely large, for two physical reasons:

(a) infinitely large values of optical thickness cannot be realised, which means there exists a maximum element number N within the set M (the set is bounded above)
(b) The number N of experiments (elements of the set M) that can be realised neither is uncountably infinite nor is it infinitely large because there is a minimum difference $(\tau_2 - \tau_1) > 0$ between optical thicknesses ,τ_1, τ_2, with $\tau_2 > \tau_1$: Optical thickness is given by an integer multiple of mean free paths, l_m. In case of infinitely large τ, $l_m = 0$, so that under this condition radiation transfer would break down completely, and the corresponding experiment could not be realised.

Accordingly, there is not only a maximum element (experiment) number N within the set M, but also the number of elements of M neither is uncountably infinite nor is it infinitely large.

Assume next that there is a very large number N of experiments each of which generates a set J of images of its corresponding events.

Theorem 2

It is not possible to create physical time scales from sets, M, each element of which generating a set, J, of images, if both the number of elements of M and of J are not *uncountably infinite*.

Proof of theorem 2

Since the number N of experiments (elements of the set M) is limited, it is sufficient to prove that each set J is not composed of an uncountably infinite number of images (this holds even if the set M of events would be infinitely large).

An uncountably infinite number of images of even an infinite number of sets of experiments or events cannot exist, otherwise there would be an uncountably infinite number of images *without* corresponding sets of events (images and events are not equipotent, and in particular, the corresponding mapping not surjective). Any set J' that comprises all images created within a specific experiment accordingly cannot not obtain the properties of the set R^+, which means, this set J' also cannot obtain the properties of physical time. The same applies to all other sets J even if an infinitely large number N of elements of sets M would be taken into account, each as origin of corresponding image sets, J. As a conclusion, while R^+ is uncountably infinite, any of the sets J, and also the total number N of sets J, and images is not. An uncountably infinite set of images cannot be generated from a finite (limited, see above) or infinitely (not uncountably infinite) large number N of elements of sets M even if each of which might create an infinitely large number of elements (images).

End of proof

We recall from Subsect. 1.3 the theorem: Physical time does not exist *a priory*, neither without space nor without events. It is the uncountably infinite number of (ordered) images that is necessary to create physical time scales. If we have only an infinite (not uncountably infinite) number of images, they do not create physical time but at the most a sequence of images (discrete instants on a *time-like* arrow) the distances of which may become infinitesimal small but are not dense in the sense the set R^+ is.

Both physical time and its arrow, in usual understanding, are created by the images of the events occurring in transparent $\mathbf{R^3}$. The first event that ever existed is probably an expansion of the universe to one Planck length, after a singularity. It is not solely this event that created physical time, but just its beginning; physical time has been created by images of *all* events that included and followed the first image. However, from theorem 1, physical time, as the image of events, cannot be created from only discrete set of events even if sets like J would contain an infinite number of images, a conclusion that follows from theorem 2 (*all* events means: an uncountably infinite large number of images).

Any set, J, of images also cannot be created from elements (images) that simply would be N-fold multiples (with N an arbitrary large element of the set of natural numbers) of the Planck time, t_P. While the number of elements of J, under this construction, indeed would become indefinitely large, the set J again would not become *uncountably* infinite, which means it is not equipotent to R^+. Though all these images are elements of R^+, the number would not comprise *all* elements of R^+.

We also cannot apply r-fold multiples of t_P with $r \in R^+$ for this construction, because only *integer* multiples of t_P ($r \in N$) could have physical meaning: Neither will non-integer multiples ($r < 1$, $r \in R^+$) of t_P exist, because no events and thus no physical time existed before completion of t_P. Nor would r-fold multiples ($r > 1$, $r \in R^+$) of fractions of t_P (as given by $r\, t_P/n$, with $n, r \in R^+$, $n \neq r$) have physical meaning because events can be correlated with physical time only if $r-1 < N <$ or $r+1$ multiples $N\, t_P$ are considered.

Physical time thus is not a set of elements that could be generated from any multiple $r\, t_P$ of the Planck time though also this set would be uncountably infinite if $r \in R^+$. Instead, only N-fold multiples (N a natural number) are possible, and this set is infinitely large but not uncountably infinite.

These results also show that considering physical time scale as the 4^{th} component of a common vector space invariably would lead to contradictions if non-transparent regions of space are involved: The structure of the three spatial and the 4^{th} time-like components, when assigning coordinates to an event e(**s**,t) in such a region, is

completely different. In the non-transparent region, and if radiative transfer is considered, lengths of the spatial vectors, **s**, are integer multiples of l_m, while time coordinates are not uniquely defined at all. Distances between events in a *4D-space-time* thus cannot be defined properly if the events occur in non-transparent space.

The results of this Subsection can be considered a special case of the well-known "inverse problems" coming up when solutions of ordinary and partial differential equations, or experimental results, shall be used to indentify the corresponding "origins", which means *known* solutions of *unknown* equations shall yield information "backwards", to identify the equations themselves and thus the underlying physical origin (that was the source for their formulation). Such problems accordingly comprise identification or reconstruction purposes as well as handling of control or design tasks. Inverse problems are frequently discussed in the literature, on mathematical and theoretical physics levels (inverse scattering, nuclear reactions) and on engineering levels (heat transfer, acoustics, seismology, chemical reactions, nano-technology, and others). For an introduction to inverse problems, compare e. g. Burger (Ref. 11) and literature cited therein.

2.4 Conclusions from theorems 1 and 2

If events exist, the *order* of their *images* in R^+, if the events occur in a non-transparent space, logically is the same as the order of the underlying events provided they are of the *same* physical experiment and if the mapping function is continuous. However, if in a non-transparent medium all events from *all* possible physical experiments are considered (provided the concept of non-transparency applies to also processes other than radiation propagation), positions of the elements of $\mathbf{Z^1}$ (or their distances among themselves on $\mathbf{Z^1}$) are, though logically ordered within *specific* physical experiments, randomly distributed if the images of *all* possible experiments are taken into account: It is an infinitely large number of series of discrete images in $\mathbf{Z^1}$ the distances of which, between any two elements of J, not necessarily must be identical; nor would images of all possible experiments necessarily coincide. The distances might be infinitesimal small, but if radiation propagation is considered, there is a minimum non-zero distance that at least amounts to ξ/c, between neighbouring images of this physical experiment. If other physical experiments are admitted, the distance might become smaller or larger.

Thus the images (elements of J) in total would be intermixed in $\mathbf{Z^1}$, by superposition of the sequences of images arising from different experiments. While each sequence (belonging to a particular experiment) is logically ordered, the total sequence (from superposition of all) might not be ordered at all, a contradiction to the properties of the completely ordered (dense) half-set R^+.

As a further conclusion from theorems 1 and 2, it is not possible to simply transfer time scales from empty to non-transparent space. Physical time exists, without inherent contradictions, if images in $\mathbf{Z_1}$ of events form a dense, ordered set of elements of uncountably infinite number, which means, if it is a continuum, in the strict mathematical sense. Instead, differences $\Delta\mathbf{s} = \mathbf{s}_2 - \mathbf{s}_1$ between vectors $\mathbf{s}_1$ and $\mathbf{s}_2$ in a non-transparent medium cannot be made arbitrarily small in a way that $\Delta\mathbf{s}$ would converge to zero; the lower limit is given by the mean free path. Time scales *outside* a non-transparent medium are uniquely ordered and the elements uncountably infinite; analogue scales, if they would exist within a non-transparent medium, neither would be dense nor uniquely ordered or uncountably infinite. The images f[e(**s**,t)] at best constitute a *time-like* sequence (a sequence of discrete elements randomly distributed on this scale). The virtual observer at position **B** cannot recognise time scales at positions, **A**, of the real observer that could be transferred to his position simply because his situation is just the reverse of the situation of observer **A**: Non-transparent curtains suspend exchange of information in both orientations of connections between positions **A** and **B**, and mapping functions of events occurring in $\mathbf{R^3}$ applied to images in J thus could not uniquely be defined: the sets R^+ and J, according to theorems 1 and 2, are not equipotent.

Since both mathematical sets, R^+ and J, are not equipotent, there would be left an uncountable infinite number of elements of R^+ that cannot coincide with elements of J. The time scales, if both existed, thus not only would be very different, but time scales within a non-transparent medium, without inherent contradictions, apparently cannot exist at all.

The same conclusion applies to invariance under time-reversal. In its strict sense, invariance cannot be confirmed; instead, reversing the order of elements within the set of images (elements of J) means reversal of just a *sequence* of a denumerably

infinite, discretely though very closely neighboured images. Since J neither is dense nor quantized, also the set (–J) constructed under this reversal neither is dense nor becomes quantized.

If we yet would accept existence of physical time scales in non-transparent media, while images in this space cannot be dense, as a consequence there are sections on this pseudo time scale that do not contain images. These sections would have to be interpreted as “holes” in physical time.

The imagination of holes in physical time has gained some interest from recently reported experiments demonstrating temporal cloaking (Ref. 12): Dispersion of an optical fibre based system is manipulated in time to initiate acceleration of the front part of a probe light beam and slowing down its rear part to create a well controlled temporal gap inside which an event occurs. Extension of the gap is in the order of 10^{-11} s. The authors explain, cloaking objects, either in space or in time, requires the manipulation of light. The question then is whether also this experiment can be explained by non-existence of physical time in non-transparent media.

3 Existence of time holes

3.1 Reconstruction of events from their images in non-transparent media

Fortunately, events e(**s**,t) in non-transparent space occur even though they are not directly observable from position **A**. Location of point **A** thus is of little importance for the following consequences (1) and (2). If the real observer stays at his original position, **A**, we have, in the notation of Figs. 2 and 3,

(1) *Before completion of the experiment:* Since the real observer cannot locate the source Q (or its primary image, the target spot at x = 0), the uncertainty Δx_{QA} experienced in $\mathbf{R^3}$ with regard to the distance between **A** and the primary image (located at x = 0) of Q, at least amounts to the thickness, D, of the slab.

(2) *After completion of the experiment and the results being reported to the real observer:* He cannot identify positions, x_k, from which the reported images, $f[(x_k)]$, were created (he knows only the elements of $\mathbf{Z^1}$). He accordingly cannot correlate images in $\mathbf{Z^1}$ with events in the non-

transparent region of $\mathbf{R}^3$. The corresponding uncertainty Δt_{QA} then is at least as large as the physical time, t_D, which a photon would need to directly travel on the line of sight through the sample. A corresponding conclusion applies for processes other than propagation of photons.

Even if the real observer would be able to exactly determine the distance between his position and image of the source (which would imply $\Delta x_{QA} \rightarrow 0$), this not necessarily eliminates also the uncertainty, Δt_{QA}, on the time scale. Length of single steps along paths like W_1 or W_2, and accordingly the total length of both paths, is only statistically determined.

While a large variety of paths is open to a photon (on a statistical distribution, in radiative transfer usuaslly descried by a scattering function), and the corresponding sets of images $f[(\mathbf{s}_k)]$ in $\mathbf{Z}^1$ all are monotonously ordered, with distances between neighbouring images that, too, are only statistically defined, it is not possible to identify from images in $\mathbf{Z}^1$ *which* specific path W was chosen by the photon. Images $f[(\mathbf{s}_k)]$ in $\mathbf{Z}^1$ are completely mixed, not differentiated to a particular path W. The real observer cannot distinguish between the corresponding open and closed circles on the axis of physical time in Fig. 3 when this scale would be reported to him after completion of the experiment. For the real observer, these positions are simply discrete images the origin of which remains completely hidden.

Any mapping function $f[(\mathbf{s}_k)]$ of events arising in non-transparent media therefore is not reversible if radiation or other physical sources, or their original images, if any, and the corresponding events initiated by the sources, are located inside or behind a non-transparent curtain.

We could replace the sources by arbitrary thermodynamic “machines” provided they initíate events (excitations of in principle arbitrary nature in a correspondingly non-transparent medium).

3.2 Time holes

The authors of Ref. 12 report an experiment of which they believe creation of a time hole in physical time was demonstrated. In non-transparent space, absence of

images would not prove non-existence of events; for this conclusion yet to hold, mapping $f^{-1}f[e(\mathbf{s},t)]$ would have to reversible, which according to the previous Subsections is not possible. In the experiment of Ref. 12, however, the space “optical fibre” usually is considered *transparent*, at least at the experimental wavelengths.

The experiment reported in Ref. 12 has some similarity with the present discussion of whether physical time exists in non-transparent space. Following the previous Sections, we may interpret the non zero-length, empty intervals between images booked in the space $\mathbf{Z^1}$ as holes, too, not in a rigorously defined physical time but between discrete and randomly distributed elements of sets J on a *time-like* axis. Following theorem 2, physical time is not defined at least within these intervals, in-between the corresponding images; that is why the intervals are empty (between their endpoints, they do not contain any images). This means, if we in such a time-like space integrate over the empty intervals between images and divide the result by the number of photons concerned, the final result equals the period of time that on the average each photon travels until it leaves the space. The extension of this period, the hole, if measured in the space $\mathbf{Z^1}$, thus is given by the uncertainty Δt_{QA}. With $\tau = 20$, the extension of this period amounts to at least about $7\ 10^{-11}$ s, a period of time of the same order as extension of the hole created in the fibre optical material in Ref. 12; the agreement of course is merely by coincidence.

But also a *structural* similarity might exist between both cases that would allow analysis and interpretation of the observation made in Ref. 12 by the results presented in the present paper. We again have to clearly separate event in space and its image in physical time.

The authors explain existence of a time hole becomes obvious when occurrence of an event experimentally initiated, within the assumed time hole, is *hidden* from an observer. The event in the present case is spectral modification of a probe beam due to an optical interaction. The quality “hidden” relies, as the authors report, on the observation that the amplitude of the event is reduced by more than an order of magnitude when the cloak is turned on. An image of this interaction event on a time axis is created by the arrival time of the probe beam (the probe beam delivers the corresponding mapping function, f). Now let in a non-transparent medium an optical

interaction event (scattering, absorption/remission) occur at a position $\mathbf{s}_1$ on an optical path, W_1. A virtual observer might approach the position $\mathbf{s}_1$ as arbitrarily close as possible, but the event also in this case most probably remains hidden, at whatever close position to $\mathbf{s}_1$ he observes the event (whether the event is really hidden depends on the spatial resolution of his detector). There is probably no image of this interaction at all, but the event, for example scattering, certainly has occurred.

The event in Ref. 12 thus is of the same class of radiative interactions and their visibility as in the present discussion, and *both* events themselves may be hidden to the corresponding observers.

The authors then conclude:

(i) If the event e(**s**,t), that is, a radiative interaction (with its image a detectable signal amplitude), does not exist or, at least, is so strongly reduced that it cannot be observed safely (is hidden) within a certain period of time (what they interpret as the time-hole), there is no image, or at the most, only an almost vanishing image f[e(**s**,t)] of this event (how in detail the event is reported and the image created by the probe beam is of little importance). We recall: Here “image” means the *arrival time* at which the full, normally expected amplitude would become observable; the mapping function, here provided by the probe beam as a vehicle, creates the arrival time. So far this is in line with the analysis of events and their images in non-transparent samples.

(ii) Since we (i. e. the authors of Ref. 12) cannot observe images (times at which *full* amplitudes should be discovered) within the said period of time (the time hole), corresponding interaction events have not occurred (“what is hidden does not exist”).

Conclusions like (ii) need clarifying discussion. A clear decision could be drawn if we go back to mapping functions, f[e(**s**,t)], introduced in Sect. 1 to describe transparency, and to theorems 1 and 2. That reversibility of functions f[e(**s**,t)] shall exist, also in the present case, entirely relies on the property of the event space (optical fibres) as being sufficiently transparent to radiation. From reverse mapping,

an event e(**s**,t) = f^{-1}f[e(**s**,t)], could be identified only under this condition. In order to fulfil this property, the mapping function would have to be bijective, the property to fulfil items (a) to (d) in Subsect. 1.1. Only in this case is a conclusion as drawn by the authors of Ref. 12 realistic. This is not the case presently. Accordingly, it remains to be shown in further experiments that the corresponding event space, the optical fibre, is completely, or somewhat relaxed, at least *sufficiently* transparent, in the sense to make mapping functions, f[e(**s**,t)], definitely bijective. Only in this case can a safe decision be drawn on success of this experiment that presently relies, strictly speaking, not on images but on *absence* of images.

The problem to some extent is similar to measurement of zero resistance of superconductors. It is not possible to arrive at exactly this result; what has been confirmed is that in induction experiments (decay of persistent currents) experimental values of the specific electrical resistance are extremely small, and the detected values have decreased steadily during the last decades.

3.3 Is the space Z^1 itself transparent?

Returning to radiation propagation in non-transparent media, at least one positive aspect has to be mentioned, however. From the enormous number of images, the real observer safely can identify the last image booked in the space $\mathbf{Z^1}$: It is given by the maximum, max[f($\Sigma\ \xi_k$)], of images that result from summations f($\Sigma\ \xi_k$) obtained when photons travel along any particular path W in $\mathbf{R^3}$ (in Fig.3, it refers to the path W_1). It is thus the largest element of $\mathbf{Z^1}$. But can the observer uniquely correlate at least *this* image with the correspondingly underlying event? Since the process of exchange of information between events e(**s**,t) and position of an observer requires a non-zero period of time, the question whether the space $\mathbf{Z^1}$ is transparent can be raised also as: Can the observer look into the past to uniquely identify the event? The answer is: No, the only information is that the image max[f($\Sigma\ \xi_k$)] correlates with events on the plane x = D, but it is not clear at which coordinate, *y*, the very last emission event, the origin of max[f($\Sigma\ \xi_k$)], has occurred on this plane (compare the coordinate axes in Fig. 3) . It is thus not possible to uniquely reconstruct the plane x = D from the results booked in $\mathbf{Z^1}$.

The same applies to reconstruction of the plane x = 0 from elements of $\mathbf{Z^1}$. Clearly, all images f[($\mathbf{s}_k$)], exist in $\mathbf{Z^1}$, regardless whether they are recognised by an external observer or not. This means also the image f(e_0) exists in $\mathbf{Z^1}$; it is booked when the photon impinges on the front side of the disk (at the target spot) and is firstly scattered or absorbed/remitted. It is thus the minimum, min[f($\Sigma\ \xi_k$)], of the discrete set of images that can be found in the space $\mathbf{Z^1}$. But there is a non-vanishing probability that following events can occur on the plane x = 0 as well. For example, the scattering or emission angle at the first interaction might redirect the photon parallel to the plane x = 0 to any position, y, so that there would be different images in $\mathbf{Z^1}$ that all have their origin from interactions (subsequent events) on the same plane.

And it applies also to all events occurring between the planes: After start of its journey from x = 0, the photon for the second time is scattered or absorbed/remitted, on a plane $x_1 = \xi \cos(\beta)$, with β the angle of emission from the front surface of the slab. Again, the angle β is only statistically defined: In a purely absorbing/remitting medium, the angle is completely arbitrary, while in a purely scattering medium, the angle is given, as mentioned, by the scattering phase function. This is another statistical quantity that according to size and electrically conducting properties of the scattering centres assigns probabilities for isotropic, forward or backward scattering. This also applies to locations $x_1 < x < D$ of all other planes and for the corresponding coordinates, y. If $\tau \rightarrow \infty$, it constitutes a set now of positions x the values of which can be indicated only as statistical quantities. In case an optical thickness $\tau \rightarrow \infty$ could be realised with any known matter (which we know is impossible), the set would be composed of an infinitely large number of images, but the number still is not uncountably infinite, as the result of theorem 2.

These results clearly indicate *non-transparency of the vector space* $\boldsymbol{Z^1}$*,* because all of the conditions (a) to (d) listed in Subsect. 1.1 are violated:

Consider again items (a) to (c): changing intensity, wavelength or position of the source just leads to different distributions of images in $\mathbf{Z^1}$, neither to uncountably infinite numbers of images nor to ordering (the different distributions in an overall view could be very similar, at best), (d) changing the transient behaviour of the source leads to a set of images that well can be identified by the real observer from

observation of the images max[f($\Sigma\ \xi_k$)], but the properties “dense” and “monotonously ordered” will not be obtained within the f($\Sigma\xi_k$)-set. For the space $\mathbf{Z^1}$ to become transparent, its elements would have to be of uncountably infinite number and ordered as monotonously increasing values, a task that is in contradiction to the properties of media non-transparent with respect to transfer of photons or of other excitations that could manifest themselves as quanta, particles or quasi-particles.[8]

In summary of Sects. 2 and 3, non-transparent media do not allow bijective mapping of events, e(s,t) to images, f[e(**s**,t)], booked on a time arrow the elements of which would be dense and ordered. The most important conclusions from Sects. 2 and 3 accordingly are:

i) Physical time does not exist in non-transparent space. And as far as it perhaps existed in some transparent sub-regions of this space:

ii) Time is not transparent.

In Sect. 5, some numerical examples shall demonstrate that the potential of a real observer to recognise and describe events in non-transparent space after a disturbance is strongly limited.

4 Entropy production in non-transparent space

Thermal conductive flux, q_{Cond} [W/m^2], is accompanied by entropy flux, S, see for example, Falk and Ruppel (Ref. 13, § 6). Assume for the moment a layer of a thermally conducting, non-transparent material with conductivity λ, thickness D and boundary temperatures $T_1 > T_2$. Using Fourier’s law of conduction, for simplicty in one dimension and under stationary conditions, $q_{Cond} = -\lambda\ dT/dx$, with $q_{Cond} = T\ (dS/dt)$, because of $dS = dQ/T$, $q = dQ/dt$, entropy production is given by

$$dS(D)/dt - dS(0)/dt = [\Delta T/(T_1\ T_2)]\ q_{Cond} > 0 \qquad (1)$$

[8] Up to this point, we have not taken into account dependent scattering. It happens if clearance between neighbouring scattering centres becomes small against wavelength of incident radiation. Dependent scattering, in a strongly simplified picture, can be interpreted as “shadowing”: One scattering centre partly shadows its neighbour thus reducing the extinction cross section of both, a property that preferentially arises in non-transparent, strongly scattering media. As a result, the corresponding mean free paths increase, but the basic conclusion remains the same as before. Though some correlation between successive scattering events becomes possible, neither an

This is the basic relation to describe entropy production in a thermally conducting medium. But we wish to treat the radiative case.

As is well known, the Rosseland radiation diffusion model (Ref. 14, the original reference source) leads to a radiative conductivity given as

$$\lambda_{Rad} = (16/3E)\, \sigma\, n^2\, T^3 \qquad (2)$$

which immediately allows to switch from the preliminary assumption of a thermally conducting medium to entropy production by diffusion of radiation: We simply replace the solid thermal conductivity, λ, by the radiative conductivity, λ_{Rad}. In Eq. (2), σ denotes the Stefan-Boltzmann constant, n the real part of the complex refractive index of the medium, E the extinction coefficient, and T is a radiation temperature that is averaged over thickness, D, of the medium. Under stationary conditions, q_{Cond} is constant. Keeping for example also T_1 constant, entropy production becomes very large if the extinction coefficient, E, goes to infinity (which means also optical thickness, $\tau = E\, D$, goes to infinity, assuming thickness D is constant). Since λ_{Rad} then becomes very small, the temperature T_2 reduces to much smaller stationary values, which in Eq. (1) also increases $\Delta T = T_1 - T_2$; the temperature profile finally becomes linear.

Each direction, δ, in which radiation propagates can be interpreted as the direction of a separate beam. Since Beer's law can be applied to all these conditions, the residual radiation $i(\tau,\delta)/i(0,\delta)$ for large τ would be reduced strongly under all beam angles, δ, against normal. Any radiative transfer in arbitrary directions in the absolutely non-transparent medium, over any, i. e. also arbitrarily short distances, thus is subject to maximum entropy production or maximum loss of information. There is maximum loss of information on any event occurring in the non-transparent slab in Fig. 3 before events and their images, of whatever physical content like time of their occurrence, have reached a real observer positioned outside the slab.

---

uncountably infinite number of images nor a monotonously increasing order of the elements of $\mathbf{Z}^1$ will be observed.

Accordingly, a medium in which *no* entropy production occurs under radiative or other transfer processes must be transparent in the sense defined by the bijective mapping functions, f[e(**s**,t)], introduced in Subsect. 1.1 (additional properties might have to be fulfilled to create the ideal case “no entropy production”). Non-transparency comes into play if information is lost during transfer processes, and the f[e(**s**,t)] no longer would be bijective.

5 Stability of a type II superconductor

In this Section, we will demonstrate that it is even not sufficient to consider only differences between the time scales t and t’ that are recognized by which the real and virtual observers. Instead, another distinction between time scale t of the virtual observer and another internal time scale, t’’, has to be made.

A superconductor is stable if it does not quench, i. e. perform an undesirable phase transition from superconducting to normal conducting state. A quench results from disturbances like conductor movement and corresponding transformation of mechanical into thermal energy, from absorption of radiation, fault currents or from momentary cooling failure. Quenching proceeds on time scales in the order of milliseconds or less. Superconducting current limiters are applied to protect electrical, medium voltage electrical circuits from damage under fault currents.

Disturbances frequently are transient, but there are also permanent disturbances like hysteretic losses. Stability against quench, and the corresponding layout of fault current limiters, has been investigated in the literature by stability models, like the simple Stekly or the more advanced adiabatic, dynamic and intrinsic stability criteria; for a survey on these analytical stability models see e. g. Wilson Ref. (15) or Dresner Ref. (16).

Stability models predict under which conditions a transport current will propagate without losses through the conductor, even under a disturbance. For this purpose, all stability models correlate disturbances with corresponding temperature evolution of the superconductor, which in turn determines evolution of critical current density. Temperature and critical current density thus depend on

(a) magnitude and duration of a disturbance
(b) heat capacity of the solid
(c) heat transfer within the conductor
(d) conductor geometry
(e) heat transfer to coolant or another conductor environment like electrical insulation or matrix materials in multi-filament conductors.

If conditions (a) to (c) and (e) are fixed, and the conductor, for example, is of cylindrical cross section, the stability models allow prediction of the maximum conductor radius, condition (d) of the above, up to which zero loss transport current can be expected.

For understanding the reaction of the superconductor with respect to a disturbance, it is thus necessary to determine the resulting internal 3D-temperature excursion, T(x,y,z,t). Almost all superconductor properties depend on temperature.

When positioning temperature sensors inside a non-transparent sample, daily laboratory experience shows that temperature fields calculated by application of Fourier's differential equation will be confirmed, at least qualitatively, provided current leads necessary for coupling the sensors to some electronic measuring device do not introduce too large errors. The real observer is right when he believes that T(x,y,z,t) inside a superconductor sample or in another solid would follow the predictions given by the solution of Fourier's equation. But the measured temperature evolution might rely on averages taken by the sensors over small, non-zero partial volumes of the sample to which the sensors are mechanically/thermally coupled.

Any sensor, if operated in a non-transparent medium as a *radiation* detector, neither resolves the paths W by which single photons travel through the sample nor can it deliver any detail about transport properties and radiation field inside the sample, except for observations within a tiny environment around its position, and (perhaps) that the observed radiation is diffuse. If operated as a *temperature* detector, besides recognising incoming conductive heat flow, it integrates also over all incoming radiation contributions, but again this information comprises only diffusely arriving radiation signals that in the sample have their origin in the very neighbourhood of the

detector. Therefore, though experimental results might confirm calculated temperature excursions, temperature sensors cannot be used to compare time scales, t and t' (and t'', see below) related to arbitrary radiation events that in a superconductor may follow from a disturbance.

5.1 No correlations between events and images

A Monte Carlo model is applied to determine spatial distribution and magnitude of a large number of internal heat sources, $Q_{int}(x,y,z,t)$, that in a sample arise from absorption of radiation bundles (Fig. 4a). The radiation bundles stem from a heat source that e. g. arises during a superconductor quench. For different solid samples (ceramics, graphite), the general method has extensively been described (Ref. 17). In the present paper, the same analysis is applied to superconductor filaments (Fig. 4b). It is not necessary to repeat in detail the calculations for this specific case, only the general principle is described in the following referring to the results reported in Ref. 17. Recursion to the superconductor will be made later.

For a general description of Monte Carlo models, the reader may consult the literature cited in Siegel and Howell (Ref. 18), Chap.18.3.

Radiation bundles may be emitted e. g. from a small volume or from a sample surface that has experienced a disturbance. Creation of a heat source (the disturbance) at physical time, t, is interpreted as the "event" that the virtual observer recognizes. The Monte Carlo calculation then yields the number of bundles, P, that hit a specific sample volume element, and thus create the distribution of follow-up heat sources, $Q_{int}(x,y,t)$, the images (since $P >> 1$ occurs rather frequently, in any of the volume elements, this is just the proof that events like these cannot be reconstructed from their images).

In the simulations, the bundles initially are emitted from part of the sample surface (a target spot and later from interior positions, after scattering and absorption/remission of each bundle. Distribution of the $Q_{int}(x,y,z,t)$ depends on extinction properties of the sample material and the angle of emission from the target spot. Magnitude of the $Q_{int}(x,y,z,t)$ depends on albedo of the material, which determines remission of residual heat pulses after each absorption event, and on the phase function of

scattering. All items to determine the $Q_{int}(x,y,z,t)$ in the present analysis are treated as random variables.

The bundles shall be emitted from the target spot, x = 0, into the sample, x > 0 (compare Fig. 4a). The target spot is created after absorption of an initial pulse from the source Q. Taking the target spot as the “source”, this simplifies the procedure as it is not necessary to explicitly take into account for exact position of an original (external) source, Q. Under radiative equilibrium, after absorption of the bundle at a mean free path, l_m, a new bundle would immediately be emitted, and the process continued until the bundle leaves the pellet or is completely absorbed.

However, the present model has to assume *non-equilibrium* conditions: The bundle is not completely absorbed after a single mean free path but scattered, or remitted at reduced energy, and the difference transformed into thermal energy and transferred to the competing heat transfer mechanism, i. e. solid thermal conduction. Accordingly, if the mean free path is small and if albedo Ω > 0, complete absorption will take place only after a large number of absorption/remission interactions in the pellet if the bundle has not left the sample before final absorption. If Ω = 1, there is no absorption at all so that the bundle leaves the pellet, with energy conserved.

It is assumed the radiation impinging on the target spot can be described without reference to a spectral distribution and that also the superconductor sample is “gray”, that is its radiative properties do not depend on wavelength. Tough both assumptions are rather crude approximations, they are sufficient for the present purpose (the spectral problem in ceramic solids has been investigated in Ref. 17).

The geometry of the Monte Carlo-model, as illustrated in Fig. 4a, is designed to allow division of the sample thickness into a number of layers. This allows modeling samples of different materials composition or thickness (increasing the number of layers means extended computation times, however). The cross section of the sample is meshed with small stepsΔx and Δy so that large number of area, and by rotation about the axis y = 0, volume elements V_{ij} (j ≤ N, i ≤ M) is created. The scattering and absorption/remission and the coupled conduction/radiation transfer problem thus is of cylindrical symmetry, with y = 0 the symmetry axis in Fig. 4a. For j

= 1, the resulting volume element is a circular disk of radius Δy, for j > 1, the V_{ij} are given as hollow cylinders the volume of which increases, though Δy = const, with square of their distance from y = 0. All volume elements have thickness Δx, for all j.

Assume that a large number K of energy bundles per unit time is emitted from the target spot in positive x-directions, each carrying the same energy quantum (confining the direction to positive x-values is by convention, otherwise we had to describe energy transfer also in regions outside the sample). The angular distribution of the bundles initially emitted from the target spot (x = 0) is assumed to be isotropic, without loss of generalization.

The investigation in Ref. 17 applied a variety of random variables specifying angular distribution of the bundles, position, y, within the target spot from which the bundles leave the pellet surface, path length that the bundle travels in the pellet between two successive scattering or absorption/remission events, a decision whether the bundle is partly absorbed or scattered, and finally the angular distribution of the emitted new bundle; this allows to specify anisotropic scattering.

For determination of temperature excursion with time in a conductive solid, Carslaw and Jaeger (Ref. 19) showed that an initial temperature distribution is equivalent to a distribution of instantaneous, initial heat sources. Conversely, once the radiative volume power sources have been determined from the Monte Carlo simulation, this distribution is equivalent to an initial temperature distribution within the pellet. At this point, coupling between radiative and conduction heat transfer in the calculations would have to be considered, and analyzing conduction total heat transfer then would again require application of Fourier's equation; this is reported in Ref. 17. But we will stop here, because application of Fourier's equation again would produce only what the real observer *believes* to have occurred inside the non-transparent sample.

Reliability of the numerical method describing multiple absorption/remission and scattering events has been confirmed by calculation of the angular distribution of directional intensity (compare Fig. 3 in Ref. 17) emitted at the rear sample surface, for different values of the extinction coefficient. This also showed that a number K = 5 10^4 bundles is sufficient for such present simulations, in agreement with radiative

Monte Carlo simulations reported in the literature (extended numbers of bundles would increase computation time, without much benefit).

In the present investigation, we are more interested in the number of absorption/remission events to be expected in the volume elements of the sample. Data reported in Ref. 17, the number P of absorption/remission (excluding scattering events), demonstrate that with the small target spot, most of the events are to be expected at forward (from x = 0) angular positions. The number of individual events per volume element ranges from a very small number at large up to several thousands events expected at small element number, respectively. This again confirms that in real situations, there is no potential to reconstruct events from their images that coincide within a simulated period of time $\Delta t = 1$ μs, at fixed time, t, within a total interval of 10 μs.

The examples in Ref. 17 also show that summation over the number of events taken from all volume elements yields a number, P, by a factor of about 10 larger than the number $K = 5\ 10^4$ of bundles. This is due to multiple scattering and absorption/remission events that a bundle experiences on is path through the sample, and it reflects the assumed albedo (on the average, $\Omega = 0.5$). If only absorption events are considered, there are about 10 absorption/remission events per bundle; if also scattering would be taken into account, the number obtained from the summation then should be a factor of 20 larger than the number K of bundles, which then would reflect the optical thickness ($\tau = 20$ mean free paths, on the average, would be expected for each bundle).

A considerable number of beams is backwards scattered from the sample and lost, or is forward or under large angles scattered in the slab and thus lost again (no deposits of energy are obtained from only scattered beams) while beam is not consumed completely during a single absorption interaction with the material. Also for this reason is reconstruction of the events not possible: The number P of images per volume element, as indicated by the symbols in Fig. 5 of Ref. 17, is large, $P >> 1$, in almost all volume elements.

The strongly inhomogeneous temperature distributions reported in Fig. 6 of Ref. 17 lead to the conclusion: While in solely *1D conductive* heat transfer, the temperature evolution at rear sample surface (x = 0) is homogeneous in space (identical for all coordinates, y), this is no longer the case in *1D coupled conductive/radiative* heat transfer. As a consequence, events (absorption/remission interactions) occurring as bombardments of volume elements by photons, at an observed frequency and their images (times, t', at which temperature evolution, T(t'), attains specific values, as an integral result of bombardment and internal radiation conduction properties) together do not allow unique reverse mapping, $f^{-1}f[e(\mathbf{s},t)]$.

5.2 Impacts on stability predictions

We now come back to the superconductor stability problem. All traditional stability models rely on solely conductive heat transfer in the superconductor solids. The impact of radiation has been included only very recently (Ref. 20) into stability calculations.

Temperature fields, T(x,y,z,t), have been calculated in Ref. 21 to solve the stability problem in NbTi and YBaCuO filaments, all embedded in suitable matrix materials. The results are shown in Figs. 5a,b.

As before, the real observer has no quantitative information about any transient states in the interior of the (non-transparent) superconductor filaments nor does he know the cause of the disturbance. The real observer could operate a detector outside the filaments in order to control, for example, surface temperature on the conductor, current flow, possibly upcoming electrical fields in the filaments that would indicate build-up of a resistive state, and other macroscopic physical quantities that can be accessed from outside positions; all this would be very difficult to measure. Most interestingly is the event "quench" because the superconductor then quickly becomes normal conducting, with corresponding consequences for its operation in an electrical grid (as announced, we may think of the sample as being part of a superconducting fault current limiter). But like the internal temperature fields, T(x,y,z,t), the event "quench" is at first instances a *local* event, $T(x,y,z,t) > T_{Crit}$, the critical temperature, a materials property, that cannot be detected by a real observer from the outside.

As before, the question is whether physical time, t', as recognised by the real observer could perhaps be uniquely correlated with physical time, t, as measured with a clock by the virtual observer operating inside the conductor. Is the real observer in a position to reconstruct events from their images like the time (the image, t') when a quench occurs? Events for the virtual observer are, as before, scattering and absorption/remission of photons but also variations of current density, due to variations of the internal temperature fields. Since absorption leads to local temperature increase, there must be corresponding reductions of local critical current density that very sensitively depends on local temperature within a superconductor. The event "quench" then could be mapped to yield images like "time at which zero-loss transport current, at positions inside the conductor, breaks down".

Ref. 20 describes results of stability calculations (stability function, zero loss DC transport current) under transient disturbances. According to the numerical method by which these results were produced, this is again what the real observer *believes* to occur in the non-transparent sample, here a superconductor. Instead of solely considering temperature fields, he believes also the critical current fields proceed according to physical laws that are differentiable, at least with respect to time. Images reported by the virtual observer are the particular times, t, at which, for example, a variation of the critical current density is *detected*; the stability function then contains the integral over the distribution of critical in relation to fault current density. The real observer has no idea by which local events a variation of the stability function was initiated. He can only make assumptions like "perhaps an increase of local transport current over critical current, or temperature above critical temperature"; such assumptions are based on the integral picture "stability function". Most importantly, he has no idea *at which time t* (as seen by the virtual observer), the *origin* of the externally observed variation of the stability function (as seen by the real observer at his time t'), was measured. The conclusion accordingly is the analogue to the end of Sect. 2:

In terms of mapping functions, time dependence of events, e(**s**,t), and their images, f[e(**s**,t)], have to be generalised to e[T(**s**,t)] and f{e[T(**s**,t)]}. A unique mapping of T(x,y,z,t)] to the field of critical current densities, J_{Crit}[T(x,y,z,t)], can be found from

usual 3D-diagrams that against the axes temperature, T, and magnetic flux density, B, describe the regions where superconductivity (non-zero critical current density) exists, see standard volumes on superconductivity). If it is accepted a variation of T(x,y,z,t) is immediately followed by a corresponding reaction of the field, $J_{Crit}[T(x,y,z,t)]$, the image on time scale of an event "variation of the stability function" would be very similar to the image of the event "variation of the temperature field". In reality, break-up of electron (Cooper) pairs and recombination also require non-zero time intervals and induce a delay in time, Δt'', see below.

Even if a transient disturbance would be distributed homogeneously in a superconductor, in particular in a plane x = 0, it is not possible to reconstruct the origin "event" from the stability function and its development in physical time. This could simply be the consequence of, for example, of a hot spot (as shown in Fig. 6 of Ref. 20) that under coupled conduction/radiation heat transfer would develop on surfaces also of a superconductor. The same applies of course to local electron pair (carrier) density, critical current density and a variety of other superconductor properties that all depend on temperature.

In summary, there again is no bijective mapping between events (variations of temperature under a disturbance, for example a fault current) and corresponding images (stability function, break-down of non-zero current transport), not only because a real observer is not able to recognise these events as internal to the superconductor, but also because physical time, t, in the non-transparent superconductor apparently does not exist, for the same reasons as outlined in Sections 2 and 3.

5.3 Relaxation time

Yet, there is still another problem with time scales. Up to now, we have implicitly assumed that there is just *one* "internal" time scale, t, as seen by a virtual observer and just *one* time scale, t', as recognized by a real observer. In standard stability analysis, decrease $dJ_{Crit}[T(x,y,z,t' > t_0')]/dt$, of critical current density (t_0' indicating start of the disturbance, on the physical time scale, t') during the corresponding warm-up period is considered to closely follow increase of local temperature in the superconductor. Local temperature, usually measured with sensors thermally

(mechanical or radiative) connected to the solid, thus reflects the "*phonon* aspect" of the transient stability problem. In reality, superconductor stability is not confined to analysis of transient conduction/radiation heat transfer. Instead, the question is whether decay of electron pairs, the "*electron* aspect" under a disturbance, and subsequent recombination of excited electron states to a new dynamic equilibrium carrier concentration, proceeds on another time scale t'' and whether *this* time scale is identical with the traditional (phononic) time scales, t or t'.

Further, normal/superconductor phase transition during warm-up or cool-down periods traditionally is considered to occur at exactly the instant when solid temperature, the output of the phonon aspect, coincides with critical temperature, T_{Crit}. Critical current density, $J_{Crit}(x,y,t)$, under the assumption t = t' then should become zero (or during cool-down return from zero to $J_{Crit}(x,y,z,t) > 0$), exactly at this instant, t. But it is not clear that during cool-down from normal conducting state, when the time, t, the temperature T(x,y,z,t) becomes less than T_{Crit}, the previously normal conducting electron system of the superconductor has already completed return to a dynamic equilibrium mixture of normal conducting and superconducting components, in a two-fluid model.

Instead, at very low temperature, the superconductor electron system is decoupled from propagation of thermal waves. It reflects its own dynamic response to this or other specific excitations, by corresponding relaxation times, τ_{El} (in the following, we will call this time a time constant, or a decay or average lifetime). Thermal diffusivity, on the other hand, determines a relaxation time, τ_{Ph}, for propagation of thermal (phonon) waves in solids after a thermal disturbance. Both relaxation times, τ_{El} and τ_{Ph}, after the same disturbance, are not necessarily identical; the lattice, if excited, behaves quite differently from the electron system though there is a correlation between both systems that couples single electrons to pairs.

A similar situation (two or more different relaxation times) arises in multi-filamentary superconductors, again after a thermal disturbance: Time constant, τ_B, for propagation of magnetic flux density, **B**, in the superconducting filaments is relatively small while thermal relaxation time, τ_{Ph}, is much larger, by orders of magnitude. The inverse of this relationship in the matrix material is of enormous importance for

obtaining stability against quench in multi-filament superconductors, in particular for high field applications.

In Ref. 21, lifetimes of thermally excited electron states have numerically been calculated from their decay rates using a sequential model with contributions (a) from an analogy to an aspect of the nucleon-nucleon, pion-mediated Yukawa interaction, (b) from the Racah-problem (expansion of an antisymmetric N-particle wave function from a N - 1 parent state; this aspect is to be observed in summations of individual decay widths to total lifetime, τ_{El}, of the excited electron system), and (c) from the uncertainty principle. The sequential model is designed to account for the retarded electron-electron interaction since the phonon, mediating this interaction, travels at finite speed. The model serves to estimate the relaxation time τ_{El} needed to reorganize the electron states to a new dynamic equilibrium that is described by an antisymmetric total wave function. Calculations have been performed in dependence of transient temperature fields (after a disturbance) that are obtained from a rigorous finite element analysis.

Calculated temperature profiles are shown in Fig. 5a,b for the NbTi and YBaCuO-filaments.

For a plot of the stability function vs. the new time scale, $t'' = t' + \Delta t'' = t' + \tau_{El}$, we calculate relaxation times for both filament samples. It is expected that the correction $\Delta t''$ to time scale t' (or time scale, t), could perhaps be strong at positions where temperature approaches T_{Crit}. This is confirmed in Fig. 6a,b that shows a plot of the delay times, $\Delta t''$, vs. real time, t, for both samples. For the NbTi-filament, a strong peak is observed near the position (x = 0, y = 0). In case of the YBaCuO-filament, there is also a sharp peak but its magnitude is much smaller so that we can as before plot the stability function vs. t' or vs. t. In the NbTi-filament, however, the delayed time, t'', locally differs strongly from real time scale t' so that critical current density, and as a result, also the stability function, if plotted against delayed time, t'', will strongly be different from the corresponding standard plots of $J_{Crit}(x,y,z,t')$, compare Fig. 7a,b, and stability function, $\Phi(t')$, Fig. 8. In this plot, the magnitudes of $\Phi(t')$ are delayed on the time axis to the proper times, t''.

Fig. 7a,b shows critical current density plotted vs. time scale (t', solid symbols) and delayed time (t'', open symbols). For the NbTi-material, the deviation is strong since the time delay, at position (x = 0, y = 0), reaches values up to 5 s. But in the YBaCuO-filament, the deviation between the curves $J_{Crit}(x= 0, y = 0,t')$ and $J_{Crit}(x= 0, y = 0,t'')$ is very small, as was to be expected.

A corresponding behaviour has to be expected for the stability function. In case of the YBaCuO-filament, there will be hardly any difference between Φ(t') and Φ(t'') but with the NbTi-filament, the deviation may be significant. It is exactly for this reason that another problem with time scales comes up:

Corrections $\Delta t'' = \Delta t''(x,y,z,t) = \tau_{El}(x,y,z,t'')$ and delayed times, $t'' = t''(x,y,z,t) = t' + \tau_{El}(x,y,z,t'')$ are different in *each* volume element of the filaments (i. e. at each arbitrary position x,y,z in the conductor) because temperature field, T(x,y,z,t'') is different in each element and so is $\tau_{El}(x,y,z,t'')$. It is therefore not possible to define a unique time scale, t' or t'', that would exactly be the same for *all* elements in any plane located close to the target spot. This excludes the usual plot of the stability function, Φ(t), in dependence of one and only one, uniquely defined time, at positions near the disturbance.

This problem becomes the weaker the larger the axial distance of the planes y from the target spot. This is demonstrated in Fig. 8: If we tentatively calculate the arithmetic mean of Φ(x,y,z,t'') taken over all elements in a single plane y, then the curves Φ(x,y,z,t'') approach the standard Φ(x,y,z,t) the more the larger the axial distance, y, from the target spot.

Stability analysis accordingly should be performed not at exactly the position y = 0 where the disturbance is located (or assumed, like a possibly developing hot spot at the superconductor/normal conductor contact in a technical application), or at distances close to this position. Instead the analysis should observe appropriate, safety related distances. These distances are correlated to propagation of the corresponding temperature field. For the NbTi-filament, the minimum distance to be observed, at the given conditions, is at least 60 µm, while it is near zero in case of the YBaCuO-filament. It is clear that the minimum distance depends on the evolution

of the particular temperature field, i. e. on the geometrical and thermal parameters (radius and material of filament and matrix, boundary conditions, diffusivity, location and magnitude of heat pulse, and others). The minimum distances thus may become larger if the temperature field looks different, e. g. under strong thermal disturbances. Note that the disturbances, Q, in the two filaments were chosen not to increase transient temperature of the finite elements (not the nodal values) above T_{Crit} (see Ref. 21 for the differences between nodal and element temperatures).

Another consequence from the different time scales, t (or t') and t'', not only affects the stability function. In a step before, it might directly concern critical current density: If under a disturbance the electron system is thermally excited, which means there is a reduction of the density of electron pairs available for zero loss transport current (or, in a magnetic field), shielding current, there could be a reduction of the magnitude of critical current density, or if critical current density is conserved, a reduction of the available conductor cross section that is open for zero loss transport. In other words, it is not clear that during the interval $\tau = \tau_{El}$'' a suffiently large number of electron pairs would (already?) be available.

As a result of the analysis, it has to be expected that temporal mismatch between relaxation times τ_{Ph} and τ_{El} creates different time scales, t (or t') and t'', of which the scale t'' is not a constant but is different in different regions of the superconductor cross section. The effect could be strong at temperatures near conductor phase transition.

Besides magnitude of critical current density and stability function, this difference could affect also measurement of observables like levitation of a superconductor in a magnetic field or results of the electronic part of the specific heat measurements, i. e. in all experiments where critical current density is concerned. The possibly existing effect has been discussed in Ref. 21 for operation also of the fault current limiter. A decrease of critical current density due to a "dead time interval", $\tau_{El} - \tau_{Ph}$, during which only a reduced number of electron pairs would be available for zero loss current transport could dangerously affect safe operation of the limiter and the electrical circuit to be protected.

6 A tempting application to current theories on the structure of the universe

Almost no quantitative information is available on extinction (scattering or absorption) properties of the universe when it rather suddenly became transparent and at times before. The mean free path of electrons in the centre of the Sun is below 1 μm, already a factor of at least 1000 smaller than assumed for the mean free path of photons in the calculation of the solid samples in Ref. 17, or in the superconductor filaments in Section 5; in a white dwarf it is several orders of magnitudes even below this value, see standard volumes on plasma physics.

Assume that the rest mass density, ρ, of the universe at times after the recombination time of $7*10^5$ years was in the order of 10^{-20} kg/m^3 (Ref. 22, Chap.10.4.4). With the specific extinction of very small, solid particles, $E/\rho = 3.3*10^{-3}$ m^2/g, at cryogenic temperatures, we have $E = 3.3*10^{-20}$ 1/m. With the radius of the universe of at least 1 Mpc (Mega-parsec) *at this time*, this results in an optical thickness of the order $\tau = 10^3$, a very rough estimate that only indicates the optical thickness probably was very large.

Provisionally assume that the distance between real observers and the opaque background is constant. Then, as a consequence from non-transparency of physical time in or behind opaque curtains, the order of the time scale between a singularity (if it existed) and the date when the temperature of the early universe had fallen to 3000 K, might be re-considered. As for a slab of non-transparent material, we have an uncertainty Δt_{QA} (like in Subsect. 3.1) that should amount to at least $3\ 10^5$ years. Within this period of physical time, a unique ordering of events within the non-transparent medium and identification of particular events including an origin of time apparently is not possible, as follows from Sects. 2 and 3. This limit exists regardless how close the horizon may be approached by observations through very large telescopes. The origin, a singularity, might exist but it is not possible to specify its exact location on the pseudo-time axis in view of this uncertainty.

Also, the distance to the horizon increases steadily. Because of the continuous expansion of the universe, more and more cosmological objects will become visible, and the densities of galaxies should increase when observations extend further in the

past. This follows from observations of radio galaxies which means the (almost) transparent, presently visible space will gradually become more and more non-transparent. Identification of such objects presently still occurs in transparent space, just outside the non-transparent background, in front of a continuously receding horizon. Problems perhaps associated with dark matter must be left open.

7 Consequences expected from the obtained results, and summary

From the theorems indicated in Sects. 1 and 2, it is not possible, in case radiative transfer in non-transparent media is involved, to create physical time in the space $\mathbf{Z}^1$ and also to clearly identify an origin of physical time in such media. Physical time apparently neither exists in minute structures like a compound nucleus, immediately after its excitation (compare Ref. 23), nor in very large cosmological spaces, if they are non-transparent to radiation. Even if physical time existed in such situations, it would not be possible to construct it in monotonously increasing order. This leads to the following consequences:

(i) It is questionable whether in non-transparent media the imagination of an origin of time, and its existence, is reasonable. This imagination rather might result from elements of psychological time. Time itself, in such media, cannot be understood in the common sense

(ii) time scales, if it is understood they are composed of an uncountably infinite, ordered set, have no physical meaning within non-transparent media, and thus cannot be transferred to these media from empty space, because unique correlation between uncountably physical time and infinitely large number of events is not possible

(iii) non-transparent systems do not create own physical time scales but discrete sequences of images; the sets may have time-like properties and dimension, and the images, in an ultimate limit, be infinitesimal closely be arranged, but are yet of less density than the set R^+

(iv) time holes might exist in non-transparent media, because of (iii): whether they might exist also in transparent space is subject to existence of bijective mapping functions

(v) physical time is not transparent, at least in non-transparent media because it contradicts the properties of the half-set R^+

(vi) causality and invariance under time-reversal could be violated in the image spaces of non-transparent media if events and observers are located in regions of different optical thickness; photons travelling along a particular path W_2 after scattering and absorption/remission interactions, could result from photons that originally travelled along a different path W_1, and differentiation from which path these photons might come is not possible

(vii) determinism might not necessarily be conserved in non-transparent media under all circumstances

(viii) non-transparent media like superconductors near phase transitions require introduction of another time scale that is not uniquely defined within the solid but depends on temperature evolution after a disturbance that in turn is different at all internal positions.

These conclusions are different from relativity principles where coordinates, lengths, velocities and coincidence depend on movement of an observer in relation to objects or on gravitational fields. Here, instead, it is the optical property of regions of space that are not empty but non-transparent to radiation, and the relaxation times observed during decay of thermal and other excitations in superconductors.

Conclusions (i) to (viii) may in a large number of experiments have little impact on obtained results, but it is clear the effects exist and could reveal their importance to what we can measure and what we are able to understand in a variety of situations. Impacts might be expected in classical physics and its mathematical formulations (differential equations), in relativity (non-stationary observers and objects located in different environments), perhaps in nuclear decay and in quantum mechanics (solutions of Schrödinger's equation, uncertainty relation, perturbation theory); this list is not complete.

As a final remark, it is well known that it is not possible, from *solely* radiative transfer experiments performed at arbitrary wavelengths, to obtain unlimitedly sharp information on the geometrical extension of solid or other objects if they are at least partly composed of *transparent* materials; such may situations arise for example when thickness of thin films or dimensions of micro-miniature electronic devices are

to be determined. Appropriate wavelengths by which the experiment is performed have to be chosen to avoid this situation, if possible. Emitted or scattered radiation intensity used as the signal to determine size of an object otherwise originates not from exactly its surface but from interior positions the distance of which from the surface is at least one, but more realistically a superposition of intensities coming from a depth of several mean free paths (the “law of darkening of the sun” is a striking example). Dimensions of the object thus become diffuse. Accordingly, size of the object can the better be determined the less its transparency.

8 References

1 R. Viskanta, M. P. Mengüç, Radiative transfer in dispersed media, Appl. Mech. Rev. 42 (1989) 241 – 259

2 H. Reiss, Radiative transfer in nontransparent dispersed media, Springer Tracts in Modern Physics 113, Springer Verlag, Berlin (1988) 174

3 H. Reiss, Radiative transfer in nontransparent dispersed media, High Temp. – High Pressures 22 (1990) 481 – 522

4 R. Kippenhahn, Light from the depths of time, Springer Verlag, Berlin (1987) 238

5 G. Nickel, Determinism - Scenes of the interplay between metaphysics and mathematics, in: R. Nagel, K. Engel, One-parameter semigroups for linear evolution equations, Springer-Verlag, Berlin (2000) 531-554

6 I. Prigogine, I. Stengers, Dialog mit der Natur, R. Piper & Co Verlag, München, 2nd ed. (1981) 285

7 F. Hund, Zeit als physikalischer Begriff, in: P. C. Aichelburg (ed.), Zeit im Wandel der Zeit, Friedr. Vieweg & Sohn, Braunschweig/Wiesbaden (1988) 178 – 192

8 G. Contopoulos, D. Kotsakis, Cosmology, Transl. by M. Petrou, P. L. Palmer, Springer Verlag, Berlin (1987)

9 H. Reichenbach, Der Unterschied von Raum und Zeit, in: P. C. Aichelburg, (ed.), Zeit im Wandel der Zeit, Friedr. Vieweg & Sohn, Braunschweig/Wiesbaden (1988) 137 - 142

10 K. J. Engel, R. Nagel, One-parameter semigroups for linear evolution equations, Graduate texts in mathematics 194 (2000)

11 M. Burger, Inverse problems, Lecture notes, Institute for numerical and applied mathematics, Westf.älische Wilhelms-Univ., Münster (Germany), winter term 2007/08

12 H. Fridman, A. Farsi, Y. Okawachi, A. L. Gaeta, Demonstration of temporal cloaking, Nature 481 (2012) 62 – 65

13 G. Falk, W. Ruppel, Energie und Entropie, Springer Verlag, Berlin (1976)

14 S. Rosseland, Astrophysik auf atomtheoretischer Grundlage, in: M. Born, J. Franck, Struktur der Materie in Einzeldarstellungen, Verlag von Julius Springer (Berlin)

15 M. N. Wilson, Superconducting Magnets, in: R. G. Scurlock (ed.) Monographs on cryogenics, Oxford University Press, New York, reprinted paperback (1989)

16 L. Dresner, Stability of Superconductors, in: St. Wolf (ed.) Selected topics in superconductivity, Plenum Press, New York (1995)

17 H. Reiss, O. Yu. Troitsky, Radiative transfer and its impact on thermal diffusivity determined in remote sensing, Horizons of World Physics 276, Nova Publ., New York (2011) 1 – 68

18 R. Siegel, J. R. Howell, Thermal radiation heat transfer, Int. Stud. Ed., McGraw-Hill Kogakusha, Ltd., Tokyo (1972)

19 H. S. Carslaw, J. C. Jaeger, Conduction of heat in solids, 2nd Ed., Oxford Sci. Publ., Clarendon Press, Oxford (1959), reprinted (1988)], pp. 256 and 356

20 H. Reiss, Radiation heat transfer and its impact on stability of a superconductor, J. Superconductivity and Novel Magnetism; in print, announced to appear in Vol 24 (2012)

21 H. Reiss, A microscopic model of superconductor stability, paper submitted to J. Superconductivity and Novel Magnetism (October 2012)

22 H. Oleak, Thermodynamik der Universums, in: Chr. Weißmantel, R. Lenk, W. Forker, D. Linke (eds.), Kleine Enzyklopädie Atom- und Kernphysik, Verlag Harri Deutsch, Thun (1983)

23 H. Reiss, O. Yu. Troitsky, A thermophysical model to numerically determine the diffusivity of highly excited nuclear matter with an instantaneous, internal pulse method, in: William A. Wakeham Festschrift. J. Chem. Eng. Data 54 (9) (2009) 2483–2497.

24 St. Whitaker, Fundamental principles of heat transfer, Pergamon Press, Inc., New York (1977)

25 W. J. Parker, R. J. Jenkins, Thermal conductivity measurements on bismuth telluride in the presence of a 2 MeV electron beam, Adv. Energy Conversion **2** (1962) 87 – 103

Appendix A1

A single, isolated radiation source is assumed in the following, or alternatively there are two independent, separate radiation sources (a double source), at different locations (double sources are not used for standard laser flash experiments). It is further assumed the single source either emits one radiative pulse (flux q = $5*10^9$ W/m^2 and of 10 µs duration) onto the surface of a slab (x = 0), or there are two pulses emitted from the *same* single radiation source, now with a flux of only 10^9 W/m^2, each with duration of 10 µs as before, but the second pulse emitted 600 s after the first. The double source shall emit a single pulse only. Propagation velocity of a radiative (conductive) wave through the medium does not depend on height of the pulses (we apply constant extinction coefficients and neglect non-linear optics).

The radiation pulses emitted by the source are directed onto a surface element (the target spot) located at the centre of the front surface. For simulation of a point source, it is sufficient that the element occupies a very small fraction (< 1%) of the whole front surface, and, with a thickness of 1 mm, a still smaller fraction of the volume of the slab. It is assumed this point source completely absorbs incident pulses emitted from the original source and thus enables us to simplify the transfer problem: The original source located at positions x < 0 need not be taken into the numerical solution scheme that is applied to only the interior ($0 \le x \le D$) of the slab.

Assume that the initial temperature of the whole slab is T_0 = 100 K (which again does not affect the general validity of the calculation as long as linear optics is concerned). Calculations of the resulting temperature excursion have been performed in 3D using for the solution of Fourier's differential equation the method of finite elements and temperature-dependent transport and material properties (radiative conductivity, λ_{Rad}, and specific heat, c_p). Because of the T^3-dependence of λ_{Rad}, the problem is strongly non-linear.

Calculated surface temperatures of the slab at target positions (τ = 0) for the one or two radiative pulses from the single source are given in Fig. A1.1 After absorption of the pulses, temperature at the irradiated target spot increases locally within 10 µs to values between 190 and 220 K. The increase with temperature of λ_{Rad} and c_p explains why the peak initiated by the second pulse in comparison to the peak from

the first pulse is not just of double height. At very large times exceeding the lengths of the abscissa after start of the experiment, the curves continue to slowly converge to their stagnation temperature. In a rough estimate, if only one pulse is absorbed, if the target spot radius amounts to, for example, 30 mm, and if the specific heat, c_p, indicated above for T = 100 K is kept constant, the final sample temperature increase would amount to less than 25 mK (it is even smaller because of the increase of c_p with temperature).

Assuming there are no thermal losses from the slab surface to the environment, how long will it take the pulses to travel to the rear side of the slab? Hopefully longer than duration of the pulse, otherwise a detector would recognise radiation not only emerging from the transport process. Second, can observers at arbitrary positions distinguish the two cases? We already know the answer: No, they cannot differentiate between the two cases because of the diffusive radiation transport process.

For comparison, there is the simple case of a sudden, permanent temperature rise ($T - T_0$), instead of a pulse, delivered at t = 0 to the surface (x = 0) of a *semi-infinite* medium. For this case, the relation $x = 3.6*(a*t)^{1/2}$, with $a = \lambda_{Rad}/(\rho*c_p)$ the radiative diffusivity, ρ the density, would allow a straightforward estimate of the physical time, t, of which the real observer believes the disturbance (if he knows there indeed was a disturbance) will have to travel until a temperature increase $(T - T_0)/100$ at a position, x > 0 could be detected (details for derivation of the relation $x = 3.6*(a*t)^{1/2}$ are found, for example, in Ref. 24, Chap 4.3). But the relaxation $x = 3.6*(a*t)^{1/2}$ relation, to all experience, holds very roughly also for a slab of *finite* thickness, a thin film. For x = 0.004 m, which is small in comparison to the total thickness of the slab, we have already t = 1115 s using $a = 1.107*10^{-9}$ m^2/s, if T = 100 K would be kept constant. Radiation in this slab obviously propagates rather slowly, a natural consequence of the large optical thickness. This is almost ten orders of magnitude longer than the duration of the pulses, a good result that serves to justify the approximations. Short, single pulses, being strongly damped, will need even more time to arrive at any position $x \leq D$ than a sudden, stepwise and constant disturbance of magnitude ($T - T_0$).

This expectation is confirmed by the transient temperatures reported in Fig. A1.2a,b following emission of one or two pulses by the single source. Data are given at target positions, $\tau = 0$, or at positions exactly opposite to the target at different optical thickness. Temperature increase at positions $\tau > 0$ is at least one order of magnitude smaller, at peak values, than observed at the surface. At $\tau = 20$, a temperature increase of$\Delta T = 0.1$ K, even one order below the $(T - T_0)/100$ criterion, is not detected before 6 hrs.

Apart from different magnitudes, hardly any difference can be seen when comparing the curves in Figs. A1.2a,b: Neither is the double peak resolved, even when assuming a rather long time delay of the second pulse (600 s), after emission of the first, nor any other significant details can be identified, although the T(t)-curve in Fig. A2b at position $\tau = 4$ (open diamonds) was calculated in small time steps between 700 and 8000 s. Real observers do not know the strength of the source, they accordingly cannot distinguish the two different cases, by observation of thermal radiation waves (temperature variations) only.

A real observer perhaps believes he could resolve both pulses (again, if he knows there were two pulses) on his time scale from positions external to the slab, if he subtracts the data in Fig. A1.2a from the corresponding data given in Fig. A1.2b. The result (Fig. A1.2c) shows the contribution by the „hidden“, second pulse when it arrives at the different positions. What the observer experiences is just a diffuse radiation intensity at $x = D$ and a temperature variation at this position of which he *believes* it is the consequence of temperature variations within the slab and because of the previously mentioned properties of the temperature field.

In case only one pulse is emitted from a double source, Fig. A1.3 shows how the original contours (top of the figure) spread, and the peak values more and more are smoothed out, if the optical thickness of the slab is increased up to $\tau = 160$ and 240 (centre and bottom of the figure, respectively). Note the extremely small temperature increase, even at peak positions, at the rear side of the slab which means the temperature distribution is almost perfectly homogeneous.

Appendix A2

Traditional literature reports values for the absorption coefficients of Corundum at room temperature and in the far infrared of about 2000 and 200 [m^{-1}], for wavelengths of 50 and 200 μm, respectively; similar values are reported for magnesium oxide at 200 μm wavelength. However, the corresponding measurements have been made with very pure substances (single crystals). When using polycrystalline materials, scattering will enormously enhance extinction. The large value of the extinction coefficient can be justified also from comparison with results obtained by application of rigorous Mie theory of scattering for a variety of spherical or fibrous particles. For example, the specific Rosseland mean, E_R/ρ, of the extinction coefficient of spherical particles (ρ denotes density of a porous sample) amounts to about 0.01 m^2/g for particle diameter d = 4 μm and a radiation temperature of 500 K, in an absorbing medium ($m_c = 2 - 10^{-3}i$, with m_c the complex refractive index), compare Ref. 2, Fig. 6.1d. This value has been applied also to Zirconia in the present calculations. Assuming that a sample poly-crystalline material consists of spherical constituents of this diameter, and $\rho = 5\ 10^3$ kg/m^3, we roughly have $E = 5\ 10^4$ [m^{-1}]; dependent scattering might to some extent reduce this value.

Appendix A3

For illustration of the multiple scattering process, Fig. A3.1 shows the number P of absorption/remission events, in the present example for a slab of 500 mm radius and 20 mm thickness. Data are obtained from a Monte Carlo-Model for different volume elements of the slab and are given for target spot radii of 15 (circles) and 50 mm (diamonds). Element volume numbers given on the abscissa are counted starting from 100 and increased up to 6000, in steps of 100. Position of elements beginning with number 100 is at a distance y = 1 mm, and beginning with number 6000 is at y = 60 mm from the axis of symmetry. Small volume element numbers accordingly indicate incidence of radiation under small scattering angles measured against the x-axis, while large volume element numbers indicate incidence under large scattering angles (note the axial symmetry).

Fig. A3.2 shows differences that arise in the *over*-temperature, $\Delta T(x,y,t) = T(x,y,t) - T_0$, at the rear sample surface (x = D) obtained for a ZrO_2-pellet (thickness 1 mm) developing under *coupled conduction/radiation heat flow* using a constant (independent of wavelength) extinction coefficient, $E = 10^4$ [m^{-1}]. Data are given at the axis of symmetry (y = 0, uppermost curve) and for positions, y > 0, of successively increasing horizontal distances (radial directions on the sample, compare Fig. 4a) in steps of 3 mm (counted from top to bottom). We have $r_T = r_p$ = 120 mm, to initiate, at t = 0, strictly 1D coupled conductive/radiative heat transfer, as assumed in the well-known Parker and Jenkins approach.

Accordingly, in case of solely solid conduction, *all* curves given in Fig. A3.2, at any position, x, within sample thickness, would coincide, which means isotropic temperature distribution within planes $0 \le x \le D$ parallel to front surface, at all times, t. However, because of the additional and anisotropic *radiation heat transfer* (superimposed onto conduction), the temperature distributions as shown in this figure are no longer isotropic but depend on the radial coordinate, y, with a “hot spot” near the origin.

Figure captions for figures in the text

Fig. 1 Schematic representation, using set theory notation, of dispersed, transparent, translucent and non-transparent media. The figure relates to a fixed wavelength of radiation propagating in these substances. The figure has two hierarchies: First, dispersed media are elements of the thick circle; accordingly, all elements outside this circle are non-dispersed (continuous) media like massive solids or liquids without formation of bubbles. Second, elements of transparent, translucent or non-transparent media are elements of the thin circles, and no elements outside these circles exist (accordingly, elements of non-transparent media are not the complement of the uppermost circle with the index “transparent” but are contained only in the lowest circle). The thin circles are ordered with respect to increasing optical thickness, τ, from top to bottom of the figure. Population of the seven sets may be as given by the following examples: (1) metallised or metallic fibres, heavily opacified, non-conducting fibres or powders, soot, graphite; (2) metals, liquids (not thin films thereof); (3) glass wool with fibre diameters large compared to wavelength of incident radiation, low density powders, aerogels, fog, snow; (4) water and other clear liquids, panes; (5) pure (not opacified) glass fibre boards, powders, particle beds, concrete, sands, dust, with particle diameters large compared with incident wavelength; region (5) indicates an intermediate region between translucent and non-transparent, both dispersed media; (6) clouds, powders, fibres with medium optical thickness; (7) the vacuum, dilute gases. Size of the areas included in the circles, in relation to each other, neither indicates frequency by which they occur in nature or in technical applications nor is size an indication for their importance. Main focus of the discussion in this paper is on the shaded regions.

Fig. 2 Vector spaces $\mathbf{R}^3$ (3-dimensional geometry) und $\mathbf{Z}^1$ (1-dimensional space of images on a physical time scale); the images result from mapping functions f[e(**s**,t)] of events e(**s**,t) taking place at locations (vectors), **s**, denoted by multiples of or combinations of basic vectors, $\mathbf{r}_k$.

Fig. 3 A disk of a non-transparent, non-conductive medium of thickness, D, a radiation source, Q (shaded circle), that emits radiation pulses of intensity, i, and a real observer at position, **A**, exterior to the non-transparent slab (all schematic).

Arrows and large half-circles (envelopes to the arrows) indicate isotropic emission of radiation from positions of the plane x = D. The small circles within the slab indicate scattering or absorption/remission events that photons or excitations other than radiative experience when travelling through the slab. In the lower part of the figure, open and closed circles arranged on the upper horizontal line denote images, f(e), of events, e, as recognised by a virtual observer if he is positioned at point **B** in the figure and if he, at the instant one of the said events is observed, books the corresponding time, t, at which this occurs on his time scale (in the text it is shown that this time scale cannot be identical to physical time). The images are obtained by application of a mapping function, f(e): open and closed circles on the upper horizontal line correspond to images obtained from events on different paths, in this example the paths W_1 and W_2. See text for more explanations. The lower horizontal line indicates a true time scale (t'), as experienced as physical time by the real observer.

Fig. 4a Schematic description of area elements and of cylindrical co-ordinate systems (x,y) and, in parallel, (i,j), for Monte Carlo and finite element calculations using arbitrary solid samples. Numbers i introduced into the area elements are counted from the symmetry axis to right ($1 \leq i \leq M$) or left directions ($-M \leq i \leq -1$); numbers j are between ($1 \leq j \leq N$), and N and M are large. Rotating the area elements around the axis of symmetry (y = 0, thick dashed-dotted line) generates hollow cylindrical volume elements. Inside the volume elements, hypothetical bundles (thick solid lines) are absorbed/remitted and/or scattered. The large full circles denote final absorption of a bundle, the smaller open circles scattering of the bundle, respectively. Bundles may escape from the sample (index Escape) after a series of absorption/remission or scattering interactions; scattering angle of bundles escaping from the sample at the rear surface (x = D) is denoted by θ. Radii r_t and r_p denote target spot and sample.

Fig. 4b Section of a superconductor filament (NbTi or YBaCuO) embedded in a matrix material (Cu or Ag, respectively). Schematic presentation (not to scale; note that the x- and y- coordinates here have been interchanged, in comparison to Fig. 4a), under cylindrical symmetry (the vertical dashed-dotted line indicates axis of symmetry). All measures are given in micrometers. Superconductor and matrix material are identified by light grey and dark grey shading, respectively. The target

area (here of radius 6 µm) is indicated by the horizontal thick, black line. Horizontal blue lines indicate planes 1 to 4 used for calculation of the stability function and of zero loss transport current, at different axial distances from the target area. The finite element mesh is schematically indicated by thin horizontal and vertical lines.

Fig. 5a Nodal temperature,T(x,y,t), obtained from a finite element simulation, at front (x = 0, y = 0) and rear positions (x = 0 or 30 µm, y = 0 and 300 µm, respectively; compare Fig. 4b) calculated for the superconducting NbTi-filament under a heat pulse absorbed at radial positions $0 \leq x \leq 6$ µm, y = 0, of $Q = 2.5\ 10^{-10}$ Ws during a period of 8 ns.

Fig. 5b Nodal temperature, T(x,y,t), in the superconducting YBaCuO-filament. Same finite element calculation as in Fig. 5a, with absorption of a heat pulse of $Q = 3\ 10^{-8}$ Ws during 8 ns.

Fig. 6a Time interval, $\Delta\tau_{El}''$, as a function of real time, t', calculated in the NbTi-filament for the element (in the finite element scheme, Fig. 4b) positioned near the central front node (x = 0, y = 0).

Fig. 6b Time interval, $\Delta\tau_{E}''_{l}$, in the superconducting YBaCuO-filament. Same calculation as in Fig. 6a.

Fig. 7a Critical current density in the superconducting NbTi-filament. Data are calculated from the element temperatures reported in Fig. 6a using Eq. (14) in Ref. 21, with the exponent n = 3/2 and are given for the element (of the finite element scheme, Fig. 4b) positioned near the central node (x = 0, y = 0). Data J_{Crit} (x,y,t) are plotted vs. real time scale, t (solid symbols) and the delayed ("shifted") time scale $t'' = t' + \Delta\tau_{El}''$ (open symbols), with the shift $\Delta\tau_{El}''$ from Fig. 6a.

Fig. 7b Critical current density in the superconducting YBaCuO-filament. Data are calculated from the element temperatures reported in Fig. 6b using Eq. (14) in Ref. 21, with the exponent n = 2 and are given for the element (of the finite element scheme, Fig. 4b) positioned near the central node (x = 0, y = 0). Data J_{Crit} (x,y,t) are

plotted vs. real time scale, t (solid symbols) and the delayed time scale t'' = t' + $\Delta\tau_{El}$'' (open symbols), with the shift $\Delta\tau_{El}$'' from Fig. 6b.

Fig. 8 Stability function, Φ(t), of the NbTi-filament, calculated using Eq. (16) in Ref. 21, under a heat pulse absorbed at radial positions $0 \leq x \leq 6$ µm, y = 0, of Q = 2.5 10^{-10} Ws during a period of 8 ns (compare Fig. 4b). The figure shows Φ(t) at planes 1 and 4 (axial distances from the target spot) of y = 0 and 56.3 µm, respectively. Data Φ(t) are plotted vs. real time scale, t (solid symbols) and the delayed time scale t'' = t' + $\Delta\tau_{El}$'' (open symbols), as a rough approximation with (provisionally) an arithmetic mean $\Delta\tau_{El}$'' of the shift $\Delta\tau_{El}(x,y,t)$'' taken over the corresponding planes.

Figures in the Appendices

Appendix A1

Fig. A1.1 Surface temperature at the target spot after absorption, on the sample surface (x = 0), of one or two successively arriving radiative pulses originally emitted from an external radiation source positioned at x < 0 (compare Fig. 4a). The pulses are each of 5 10^9 W/m^2 flux density and of 10 μs duration. The target spot by its dimensions can be interpreted as a point source relative to sample geometry and size. Emission of the two pulses from the sample surface is separated by a time interval of 600 s. Results are calculated using 3D Finite Element simulation for a flat, quadratic sample (side length 1 m, thickness 20 mm) of optical thickness τ = 20.

Fig. A1.2a-c Transient temperatures at positions exactly opposite to the target spot, at different geometrical, i. e. optical thickness, for the same slab as before, calculated for one (Fig. A1.2a) or two radiation pulses (Fig. A1.2b); flux density, separation and duration as are the same as in Fig. A1.1. After subtraction of the data of Fig. A1.2a from those of Fig. A1.2b, the contributions by the second pulse can be identified (Fig. A1.2c). Open diamonds, squares, triangles and circles denote x = 4, 8, 12 and 16 mm, full diamonds are at x = 20 mm, respectively; using an extinction coefficient of 1000 1/m, these symbols correspond to optical thickness τ = 4, 8, 12, 16 and 20.

Fig. A1.3 Temperature fields given as contour diagrams taken at target position (τ = 0) after t = 10 μs (upper diagram) and at the rear side of the slab (τ = 160 and 240, lower diagrams, from top to bottom) after t = 20 hrs, resulting from a double radiation source with a centre to centre distance of 20 mm located on the front surface (τ = 0) of the slab each delivering a pulse of 10^9 W/m^2 and 10 μs duration. Like in Fig. A1.1, the double radiation source is created from absorption of corresponding radiation pulses emitted by external radiation sources. The horizontal bar indicates temperature intervals to the top figure only (target position). Maximum temperature variation at τ = 160 and 240 (lower diagrams) is 0.5 mK counted in steps of 100 μK (neighbouring colours) and 0.01 mK (in steps of 2 μK), respectively.

Appendix A3

Fig. A3.1 Number P of absorption/remission events in a slab of 500 mm radius and 20 mm thickness occurring within a period of time Δt = 1 μs (within the total interval of 10 μs), vs. volume element number, after a pulse of 5 10^9 W/m^2 is emitted from the target spot. Data are obtained from a Monte Carlo-Model for different volume elements of the slab and are given for target spot radii of 15 (circles) and 50 mm (diamonds). Extinction coefficient E = 10^3 1/m, albedo of single scattering, Ω_c = 0.5, and anisotropy factor, m_S = 6, are constant. Element volume numbers given on the abscissa are counted starting from 100 and increased up to 6000, in steps of 100. Position of elements beginning with number 100 is at a distance y = 1 mm, and beginning with number 6000 is at y = 60 mm from the axis of symmetry (compare Fig. 4a). Small volume element numbers accordingly indicate incidence of radiation under small scattering angles measured against the x-axis, while large volume element numbers indicate incidence under large scattering angles (note the axial symmetry).

Fig. A3.2 Rear sample surface (x = D) over-temperature, $\Delta T(x,y,t) = T(x,y,t) - T_0$, of the ZrO_2-pellet (thickness 1 mm) developing under coupled conduction/radiation heat flow using a constant (independent of wavelength) extinction coefficient, E = 10^4 [m^{-1}]. Initial temperature is indicated by T_0 = 300 K. Albedo of single scattering, Ω_c, and anisotropy factor, m_S, also are constant, Ω_c = 0.5, m_S = 2. The thermal diffusivity amounts to a = 5.75 10^{-7} m^2/s), near room temperature (RT), taken as constant and isotropic. Index of refraction is n = 2. The pellet is exposed to an energy pulse of 1 J delivered during 8 ns to the target spot; total incident power thus is Q = 1.25 10^8 W, like in Ref. 17. Data are given at the axis of symmetry (y = 0, uppermost curve) and for positions, y > 0, of successively increasing horizontal distances (radial directions on the sample, compare Fig. 4a) in steps of 3 mm (counted from top to bottom). We have $r_T = r_p$ = 120 mm, to initiate, at t = 0, strictly 1D coupled conductive/radiative heat transfer, as assumed in the traditional Parker and Jenkins approach (Ref. 25). In case of solely solid conduction, all curves given in Fig. 6, at any position, x, within sample thickness, would coincide, which means isotropic temperature distribution within planes $0 \le x \le D$ parallel to front surface, at all times, t.

Fig. 1

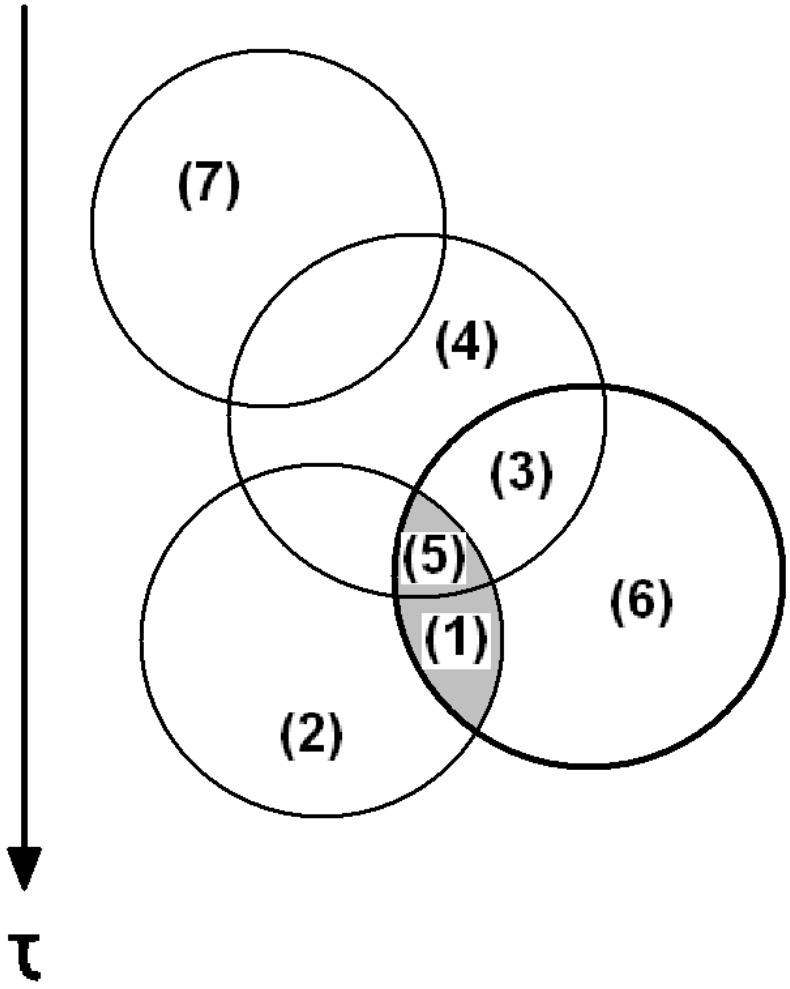

Fig. 2

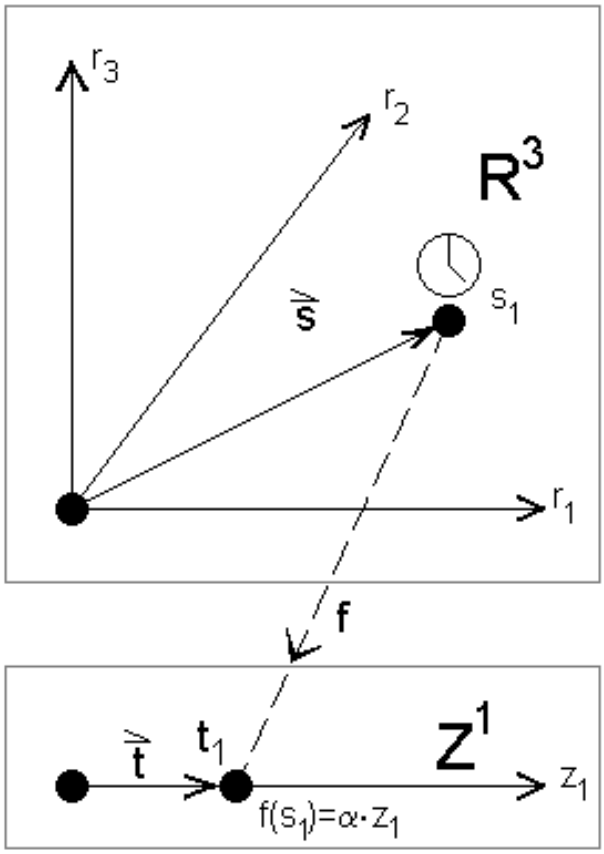

Fig. 3

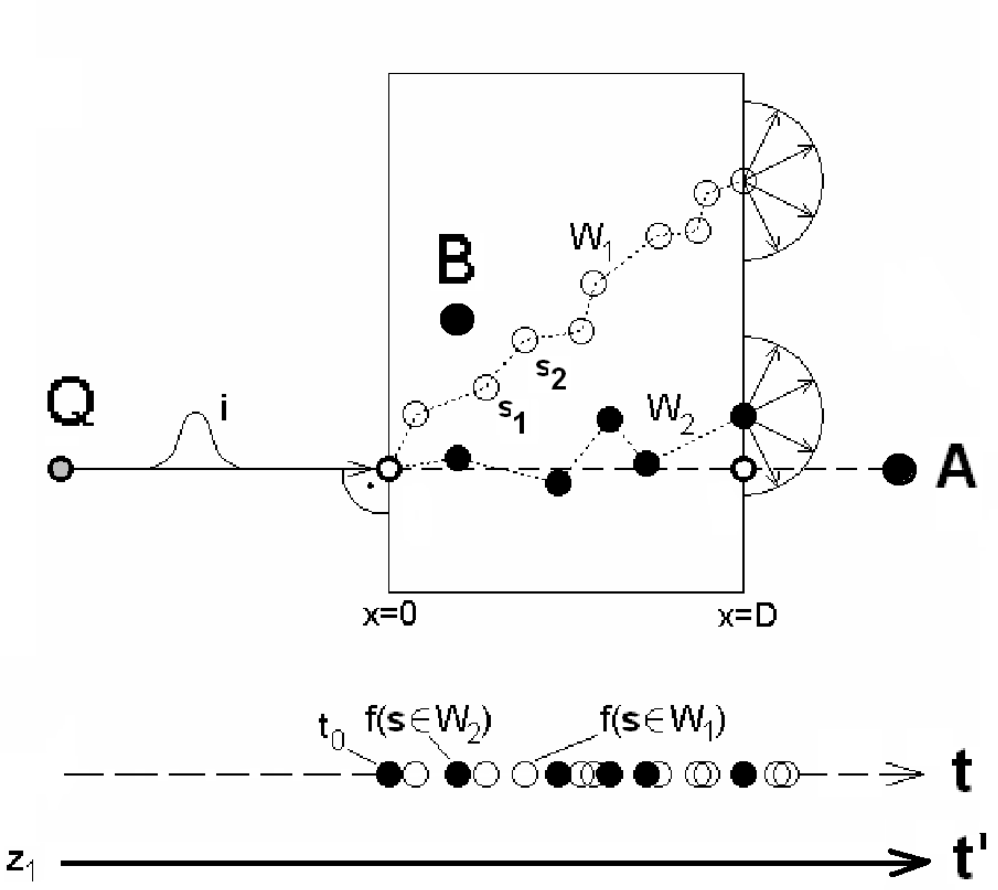

Fig. 4a

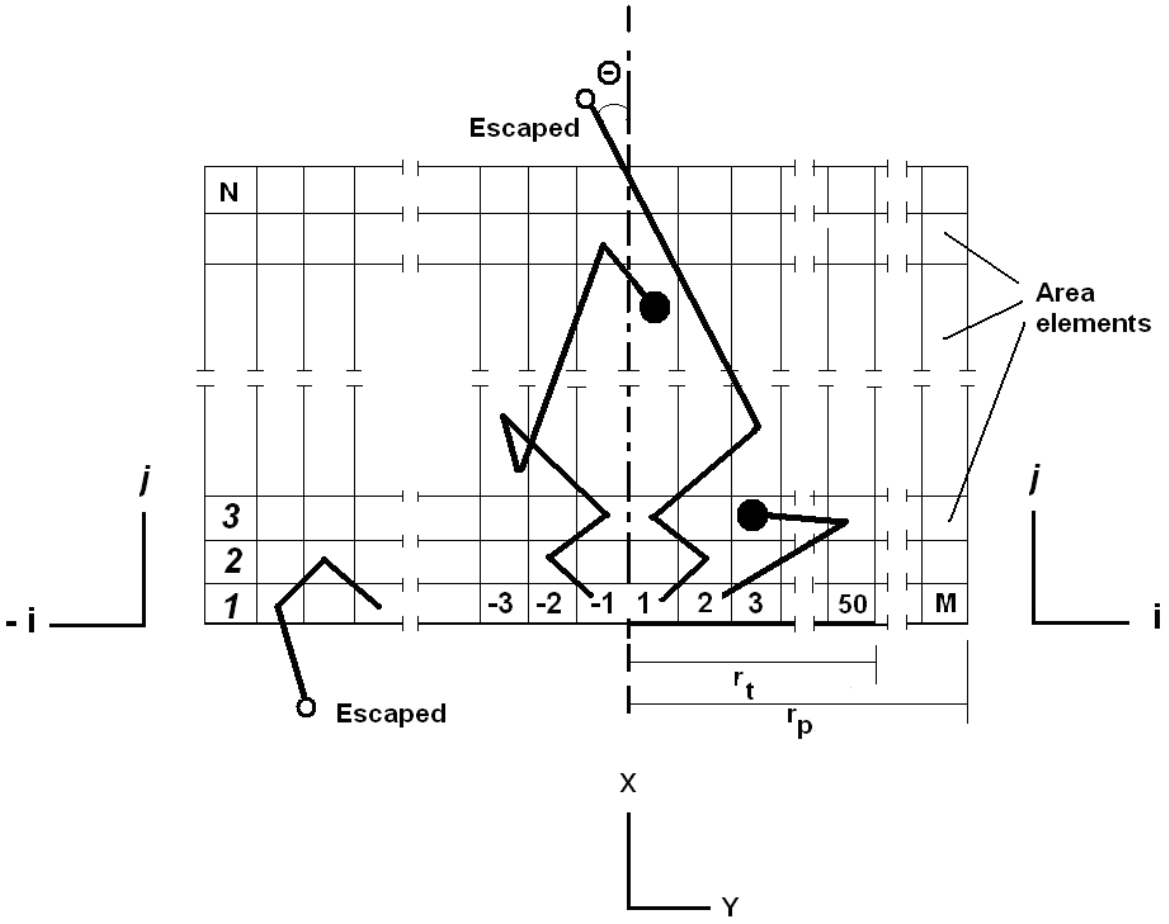

Fig. 4b

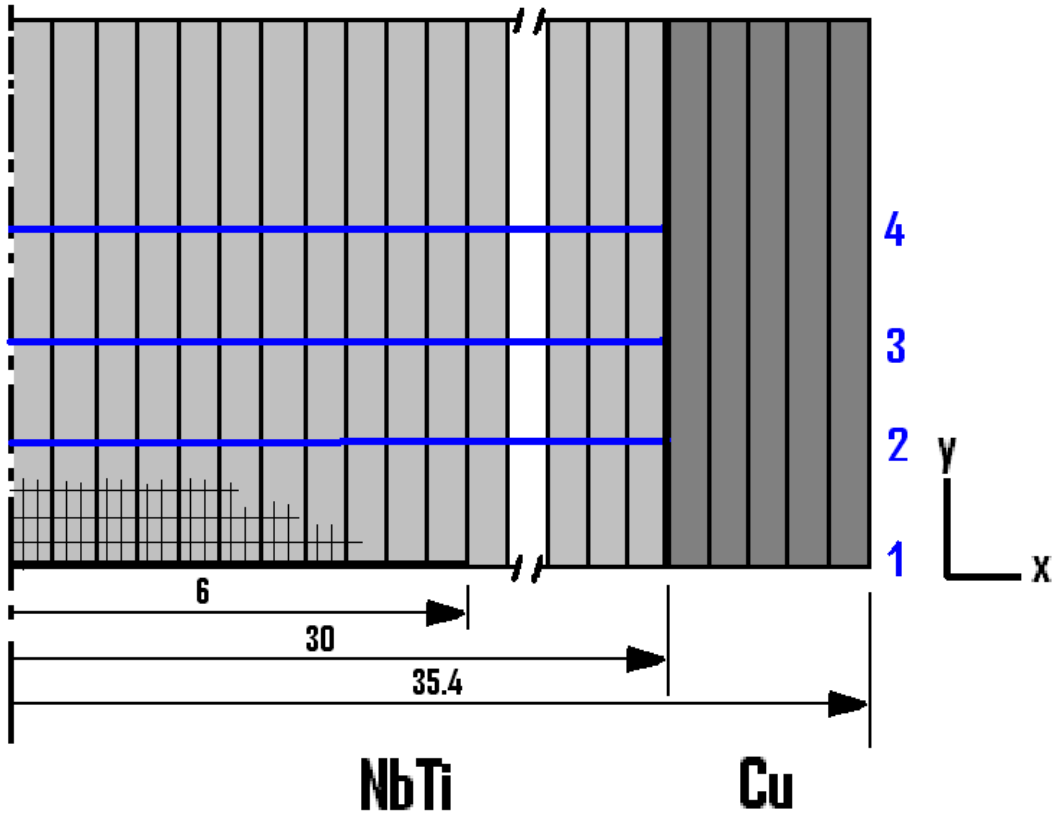

Fig. 5a

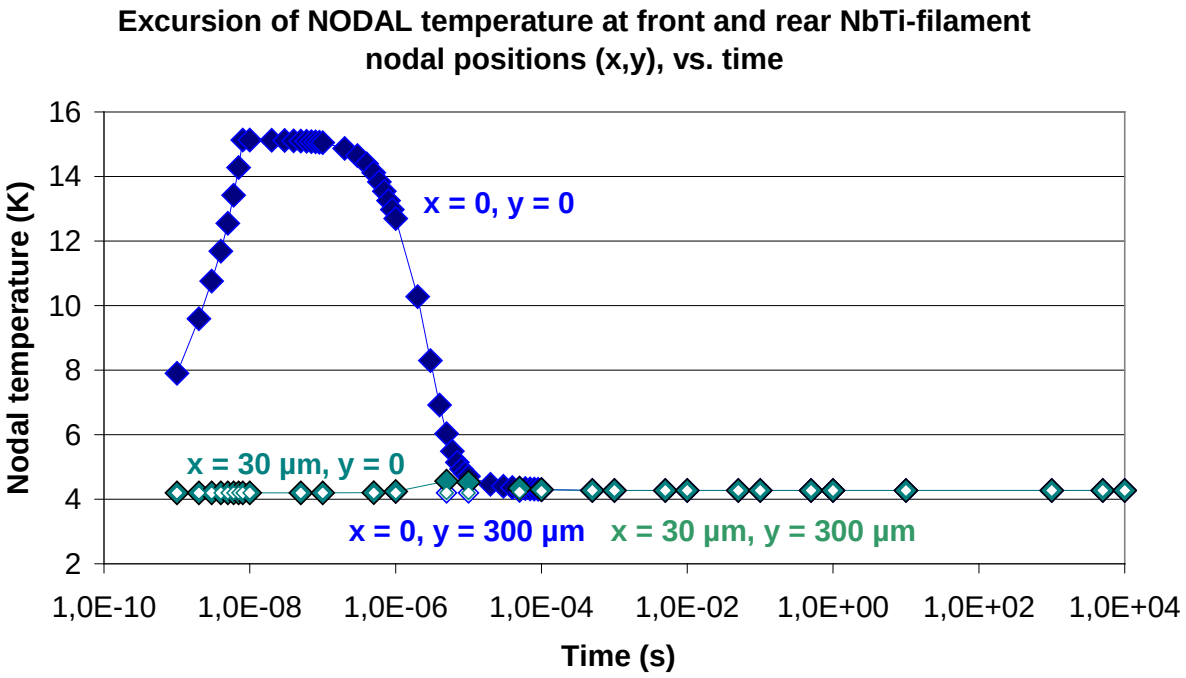
Excursion of NODAL temperature at front and rear NbTi-filament nodal positions (x,y), vs. time
Nodal temperature (K)
16
14
12
10
8
6
4
2
x = 0, y = 0
x = 30 µm, y = 0
x = 0, y = 300 µm
x = 30 µm, y = 300 µm
1,0E-10
1,0E-08
1,0E-06
1,0E-04
1,0E-02
1,0E+00
1,0E+02
1,0E+04
Time (s)

Fig. 5b

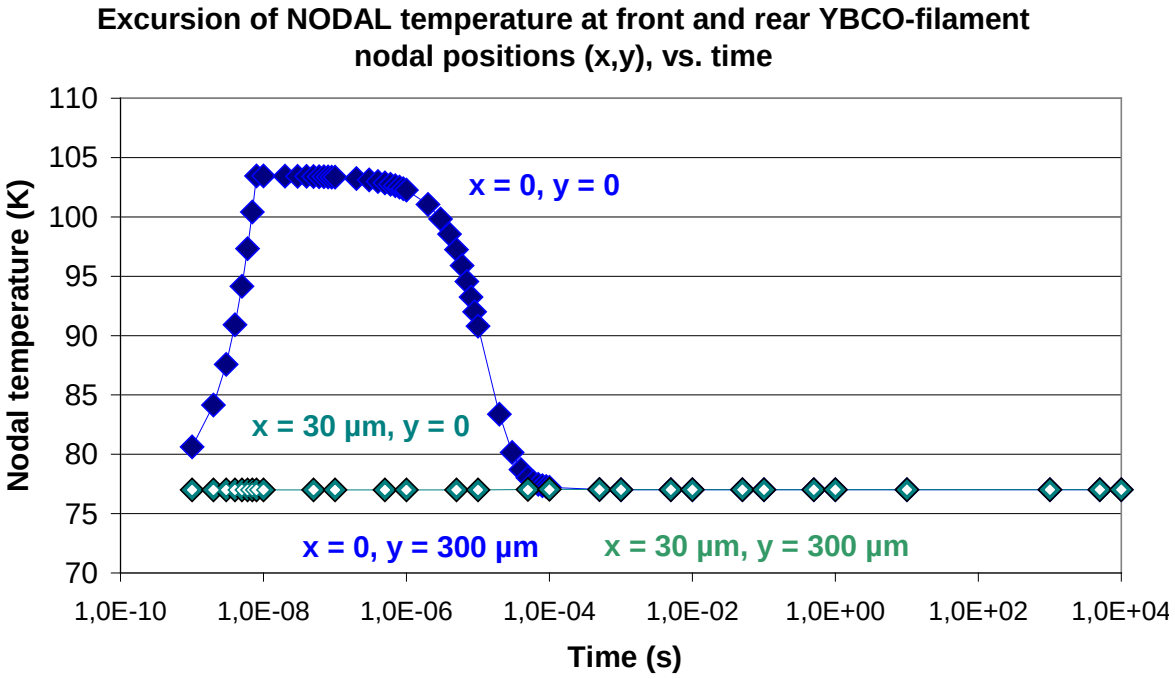
Excursion of NODAL temperature at front and rear YBCO-filament nodal positions (x,y), vs. time
Nodal temperature (K)
110
105
100
95
90
85
80
75
70
x = 0, y = 0
x = 30 µm, y = 0
x = 0, y = 300 µm
x = 30 µm, y = 300 µm
1,0E-10
1,0E-08
1,0E-06
1,0E-04
1,0E-02
1,0E+00
1,0E+02
1,0E+04
Time (s)

Fig. 6a

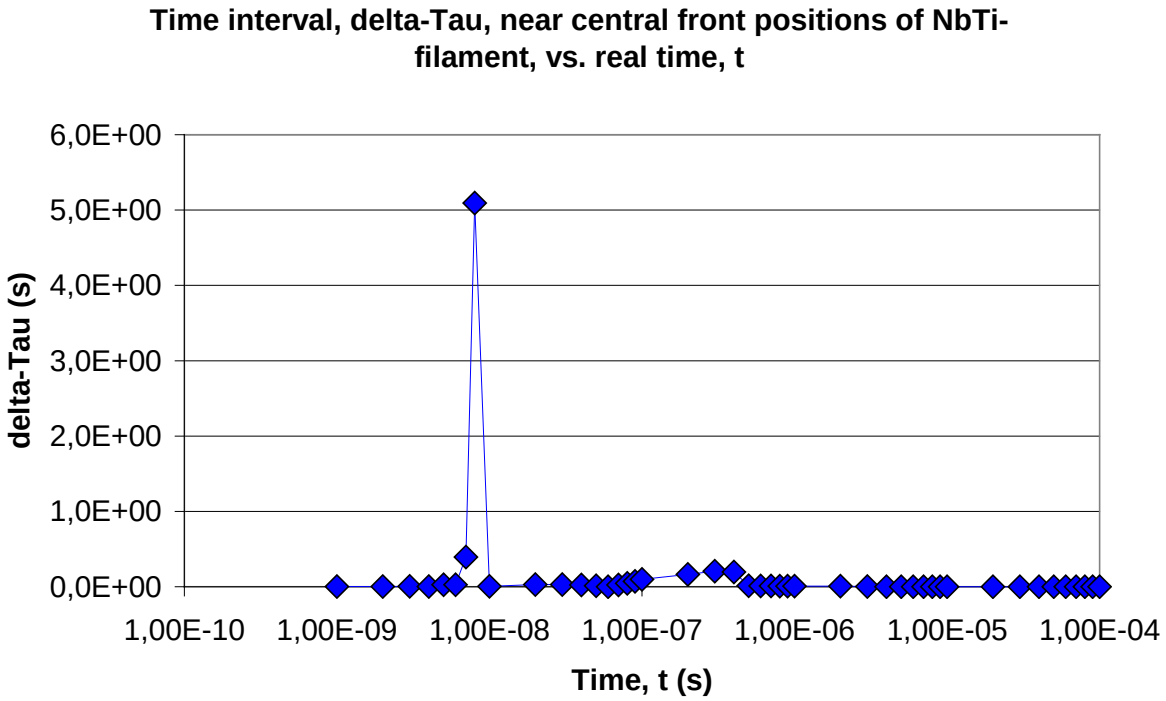
Time interval, delta-Tau, near central front positions of NbTi-filament, vs. real time, t
6,0E+00
5,0E+00
4,0E+00
3,0E+00
2,0E+00
1,0E+00
0,0E+00
delta-Tau (s)
1,00E-10
1,00E-09
1,00E-08
1,00E-07
1,00E-06
1,00E-05
1,00E-04
Time, t (s)

Fig.6b

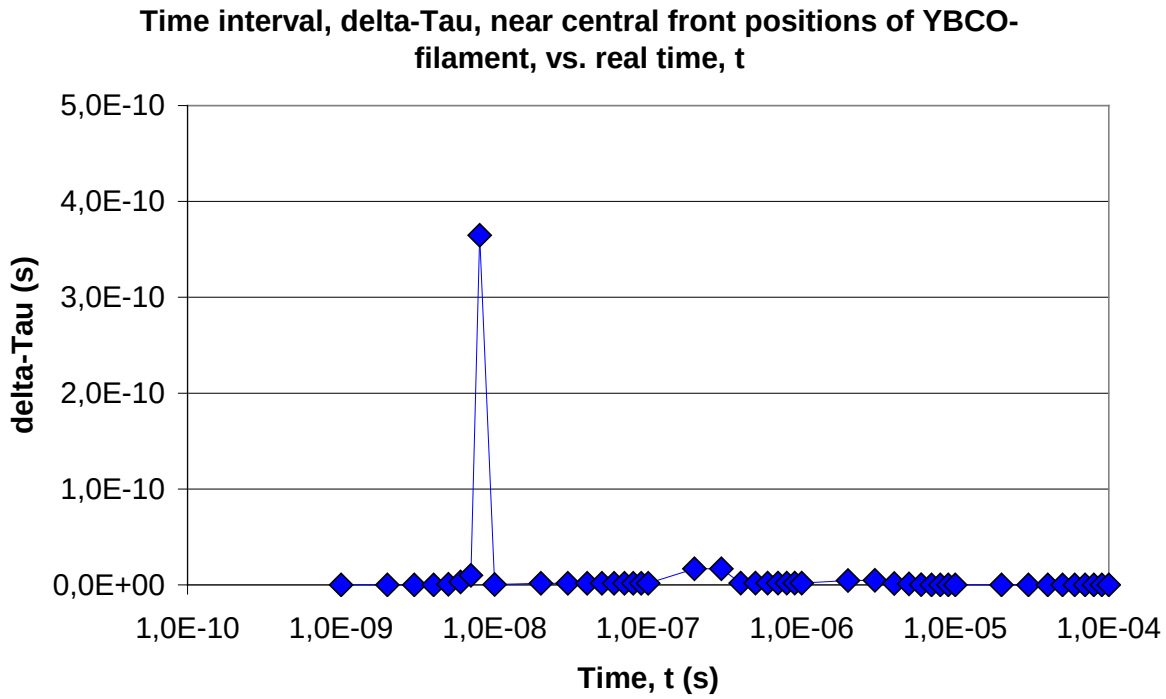
Time interval, delta-Tau, near central front positions of YBCO-filament, vs. real time, t
5,0E-10
4,0E-10
3,0E-10
2,0E-10
1,0E-10
0,0E+00
delta-Tau (s)
1,0E-10
1,0E-09
1,0E-08
1,0E-07
1,0E-06
1,0E-05
1,0E-04
Time, t (s)

Fig.7a

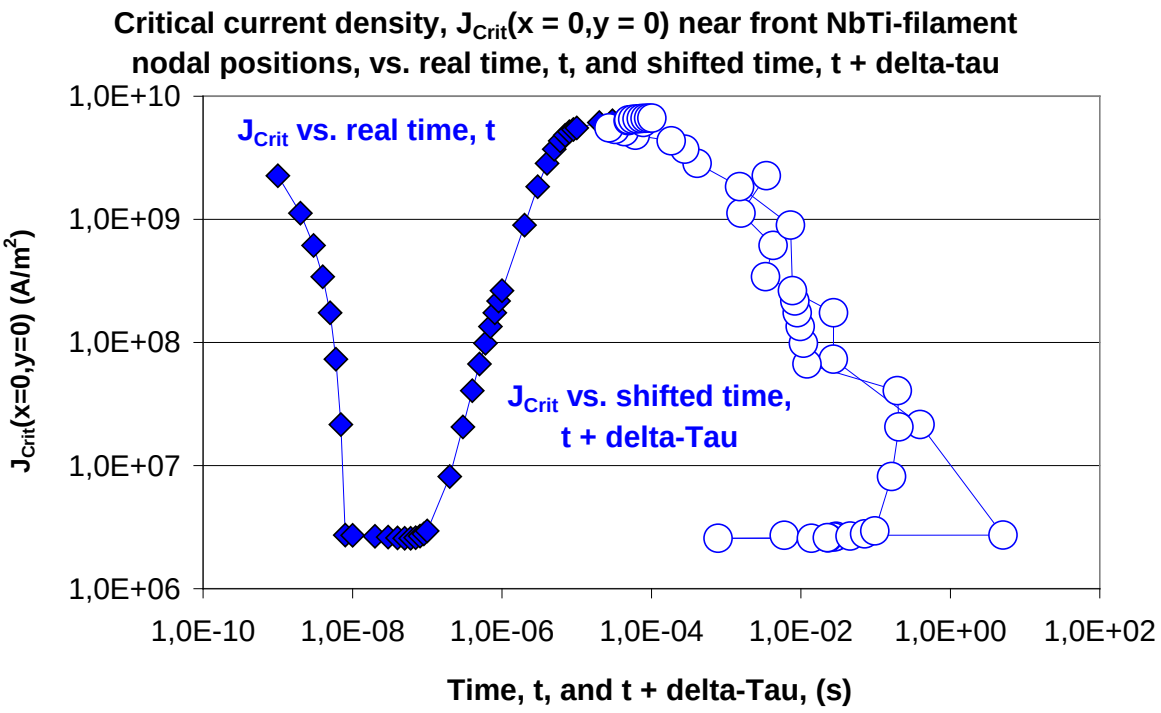
Critical current density, J_Crit(x = 0,y = 0) near front NbTi-filament
nodal positions, vs. real time, t, and shifted time, t + delta-tau
J_Crit vs. real time, t
J_Crit vs. shifted time,
t + delta-Tau
J_Crit(x=0,y=0) (A/m²)
1,0E+10
1,0E+09
1,0E+08
1,0E+07
1,0E+06
1,0E-10
1,0E-08
1,0E-06
1,0E-04
1,0E-02
1,0E+00
1,0E+02
Time, t, and t + delta-Tau, (s)

Fig.7b

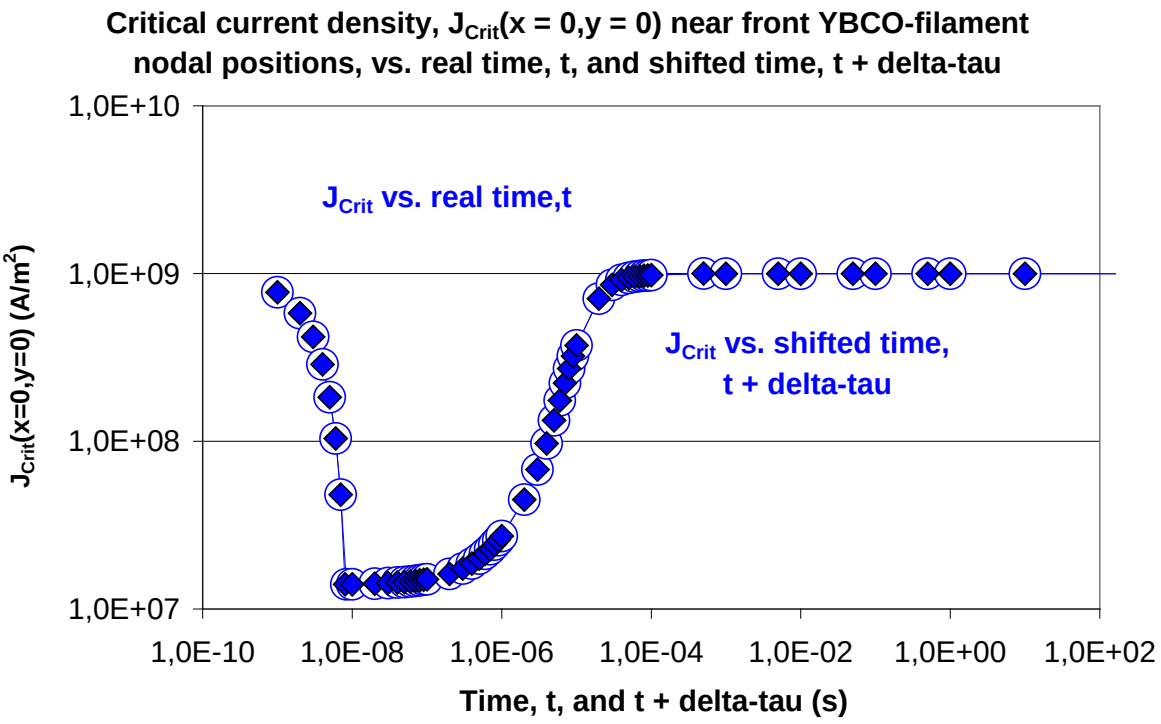
Critical current density, J_{Crit}(x = 0,y = 0) near front YBCO-filament
nodal positions, vs. real time, t, and shifted time, t + delta-tau
1,0E+10
1,0E+09
1,0E+08
1,0E+07
J_{Crit}(x=0,y=0) (A/m^2)
J_{Crit} vs. real time,t
J_{Crit} vs. shifted time,
t + delta-tau
1,0E-10
1,0E-08
1,0E-06
1,0E-04
1,0E-02
1,0E+00
1,0E+02
Time, t, and t + delta-tau (s)

Fig. 8

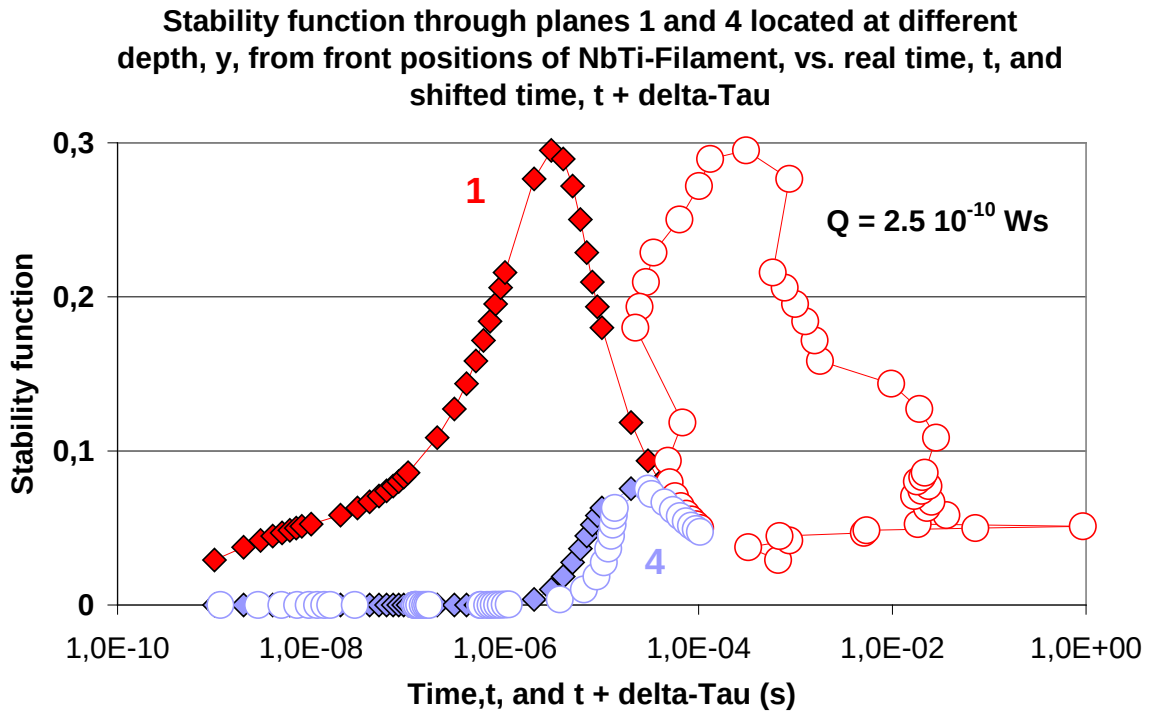
Stability function through planes 1 and 4 located at different depth, y, from front positions of NbTi-Filament, vs. real time, t, and shifted time, t + delta-Tau
Stability function
0,3
0,2
0,1
0
1
4
Q = 2.5 10-10 Ws
1,0E-10
1,0E-08
1,0E-06
1,0E-04
1,0E-02
1,0E+00
Time,t, and t + delta-Tau (s)

Fig. A1.1

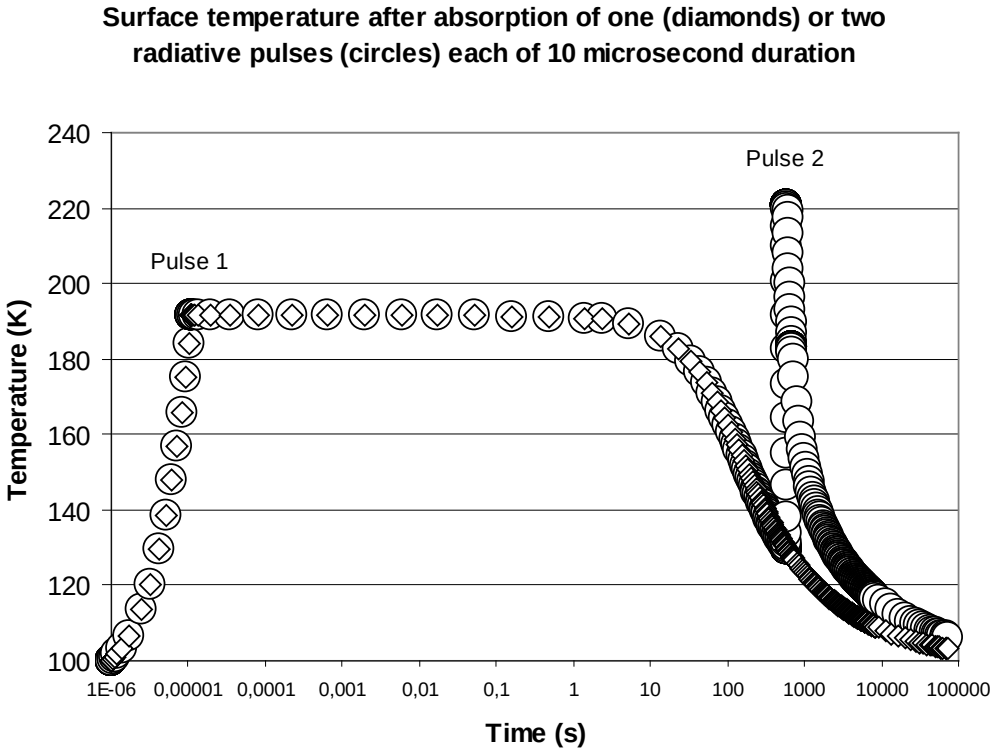
Surface temperature after absorption of one (diamonds) or two radiative pulses (circles) each of 10 microsecond duration
Pulse 1
Pulse 2
Temperature (K)
240
220
200
180
160
140
120
100
1E-06
0,00001
0,0001
0,001
0,01
0,1
1
10
100
1000
10000
100000
Time (s)

Fig. A1.2a

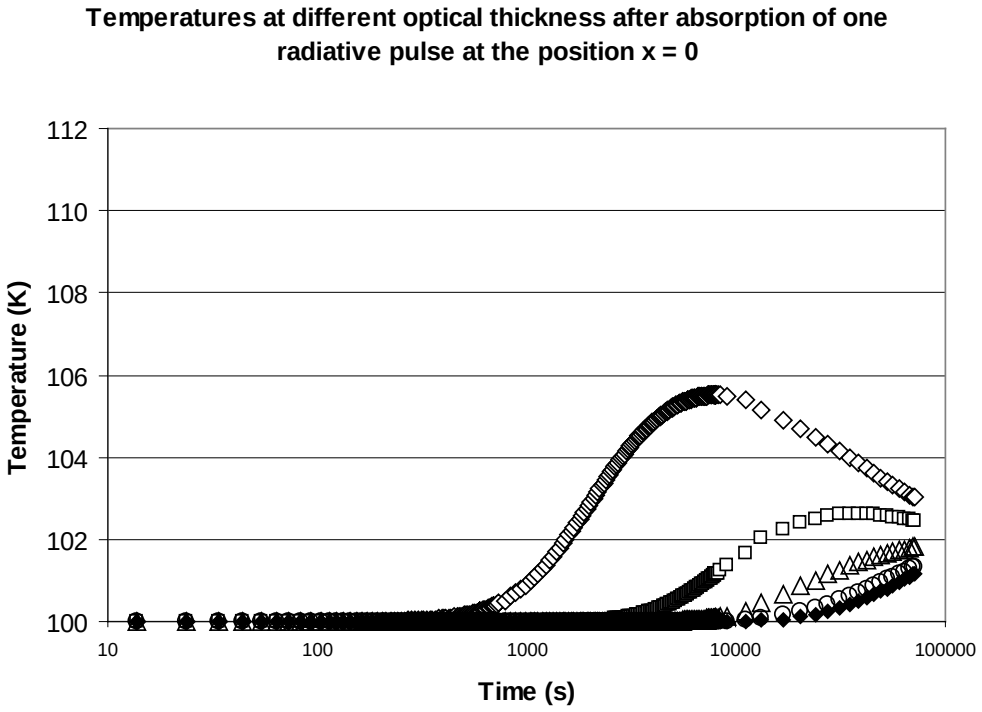
Temperatures at different optical thickness after absorption of one radiative pulse at the position x = 0
Temperature (K)
112
110
108
106
104
102
100
10
100
1000
10000
100000
Time (s)

Fig. A1.2b

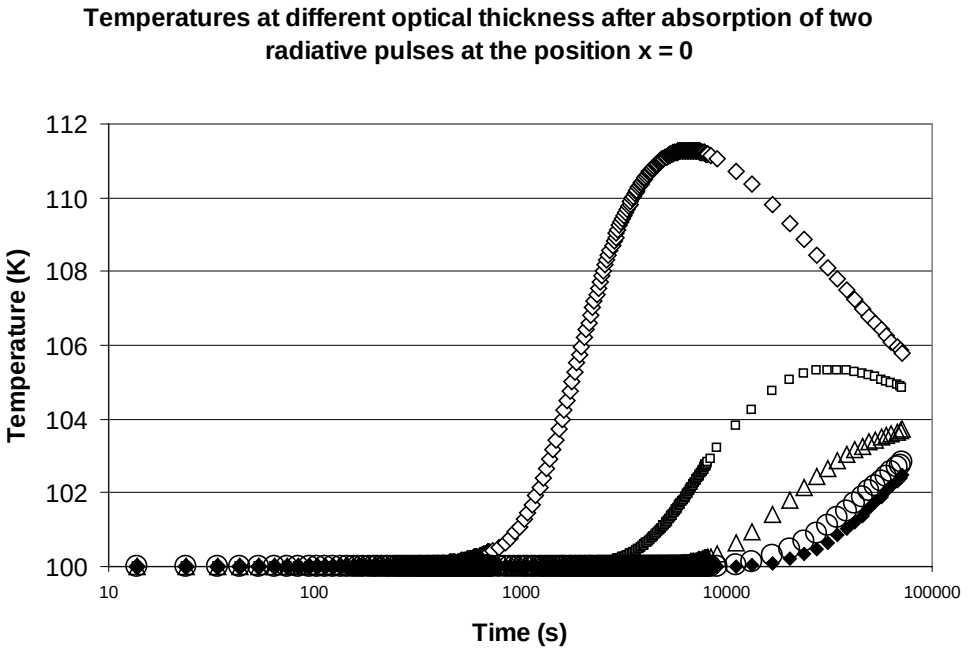
Temperatures at different optical thickness after absorption of two radiative pulses at the position x = 0
Temperature (K)
112
110
108
106
104
102
100
10
100
1000
10000
100000
Time (s)

Fig. A1.2c

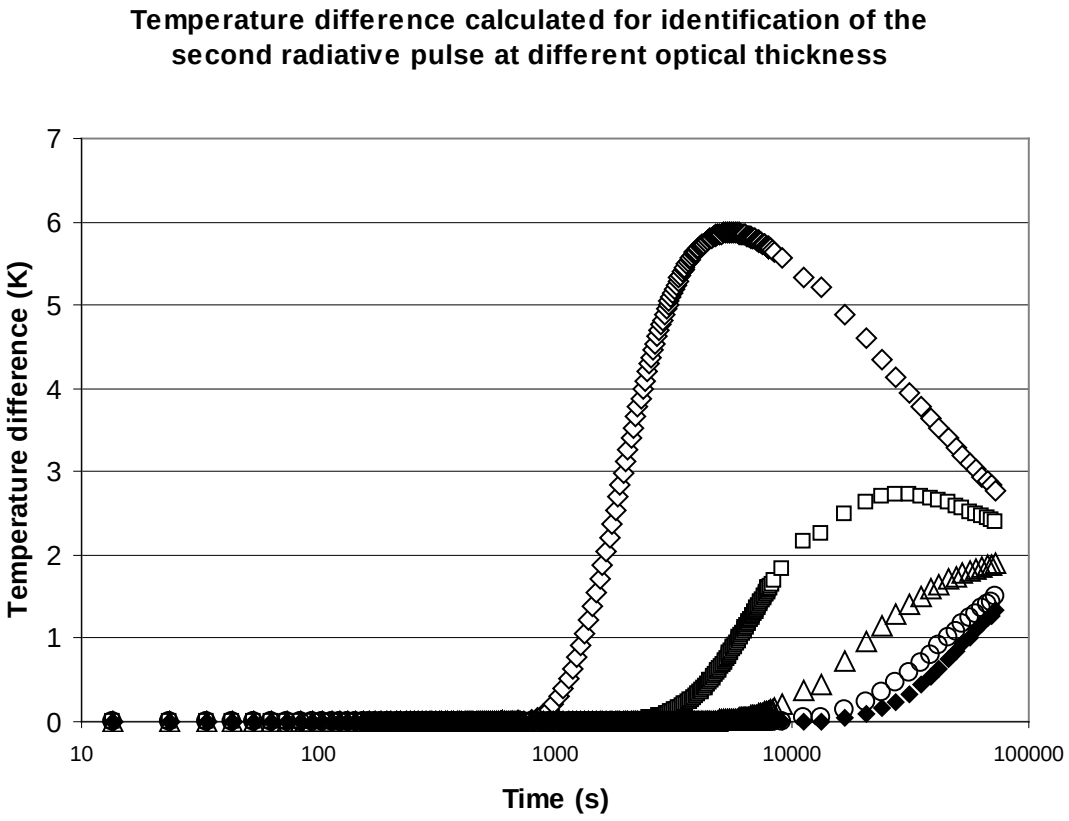
Temperature difference calculated for identification of the second radiative pulse at different optical thickness
Temperature difference (K)
0
1
2
3
4
5
6
7
10
100
1000
10000
100000
Time (s)

Fig. A1.3

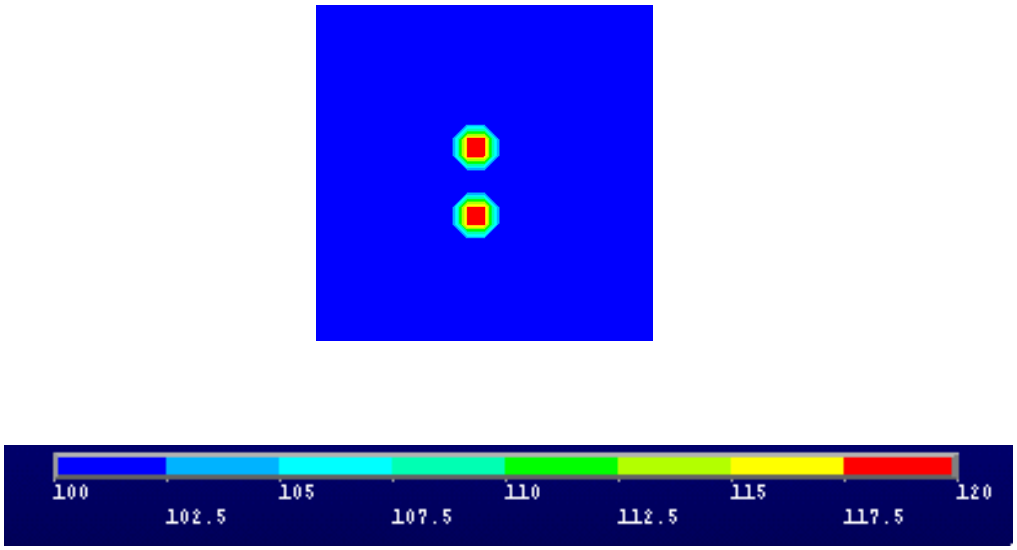

Fig. A3.1

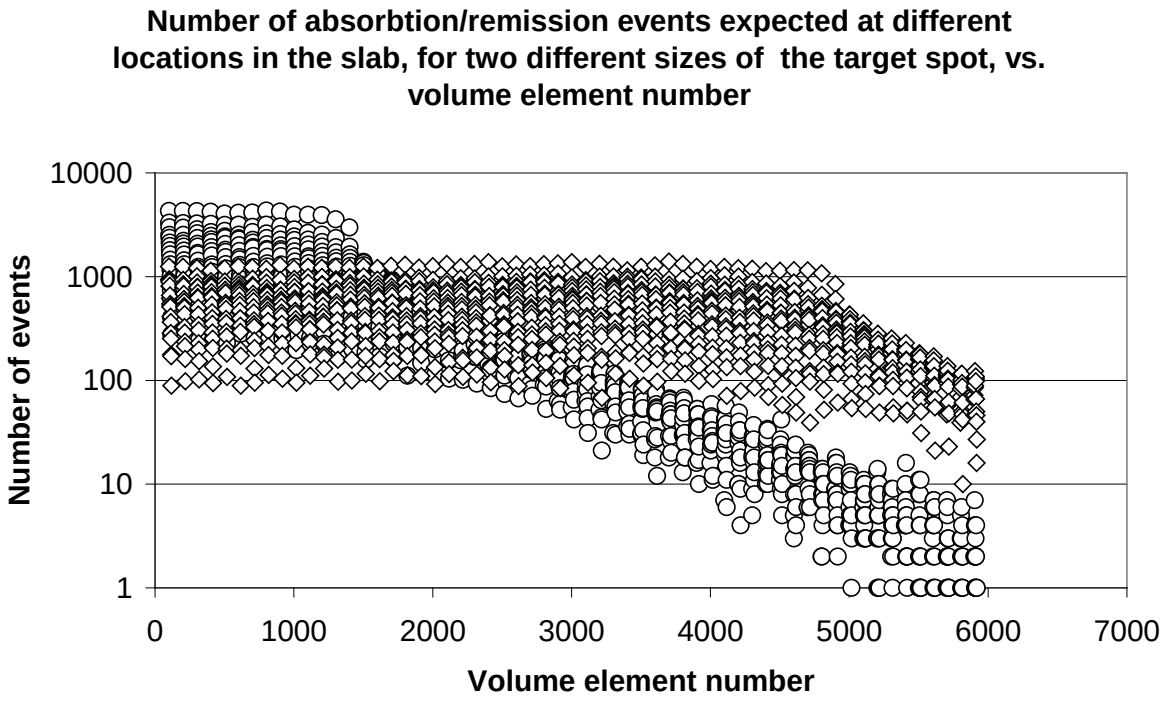
Number of absorbtion/remission events expected at different locations in the slab, for two different sizes of the target spot, vs. volume element number
Number of events
10000
1000
100
10
1
0
1000
2000
3000
4000
5000
6000
7000
Volume element number

Fig. A3.2

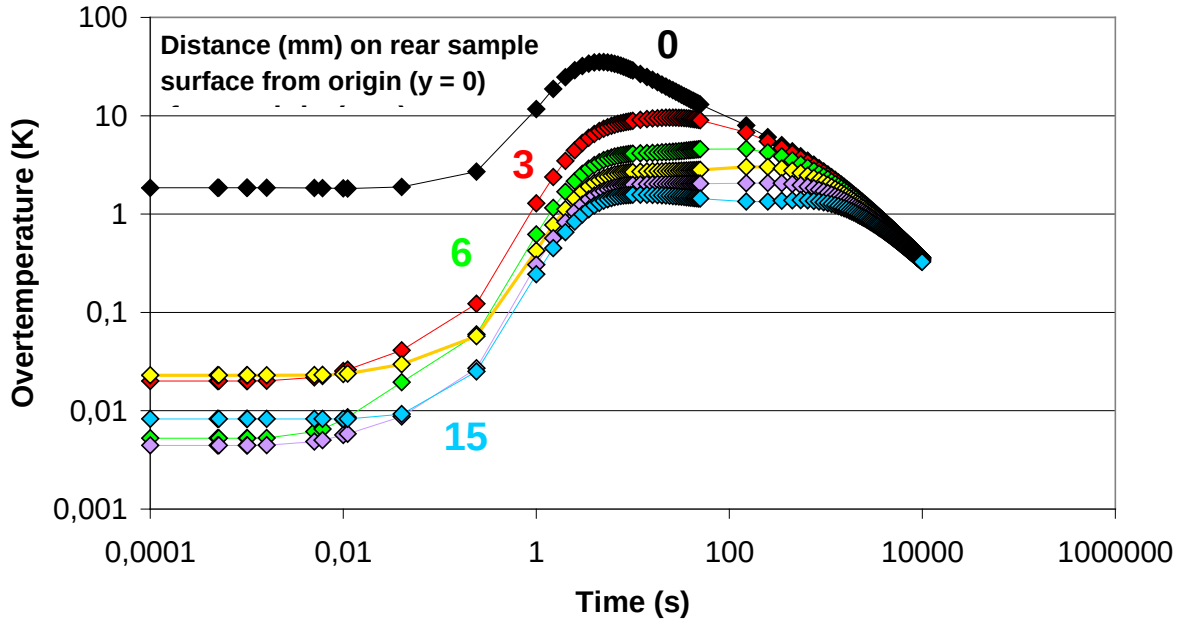
Distance (mm) on rear sample surface from origin (y = 0)
0
3
6
15
Overtemperature (K)
100
10
1
0,1
0,01
0,001
0,0001
0,01
1
100
10000
1000000
Time (s)